McMaster University
DigitalCommons@McMaster

Open Access Dissertations and Theses | Open Dissertations and Theses

4-1-2012

The Effect of Goblet Cell Metaplasia On Airway Barrier Integrity

Christopher J. Dalle Ave
McMaster University, cdalleave@hotmail.com

Follow this and additional works at: http://digitalcommons.mcmaster.ca/opendissertations

Part of the Biological Phenomena, Cell Phenomena, and Immunity Commons, and the Circulatory and Respiratory Physiology Commons

Recommended Citation
Dalle Ave, Christopher J., "The Effect of Goblet Cell Metaplasia On Airway Barrier Integrity" (2012). *Open Access Dissertations and Theses.* Paper 6554.

This Thesis is brought to you for free and open access by the Open Dissertations and Theses at DigitalCommons@McMaster. It has been accepted for inclusion in Open Access Dissertations and Theses by an authorized administrator of DigitalCommons@McMaster. For more information, please contact scom@mcmaster.ca.

GOBLET CELLS AND AIRWAY BARRIER INTEGRITY

THE EFFECT OF GOBLET CELL METAPLASIA ON AIRWAY BARRIER INTEGRITY

By

CHRISTOPHER J DALLE AVE, B.Sc.

A Thesis

Submitted to the School of Graduate Studies

In Partial Fulfillment of the Requirements for the Degree

Master of Science

McMaster University

© Copyright by Christopher Dalle Ave, November 2011

McMaster University, Hamilton, Ontario

MASTER OF SCIENCE (2011)

Medical Sciences – Physiology and Pharmacology

TITLE: The Effect of Goblet Cell Metaplasia on Airway Barrier Integrity

AUTHOR: Christopher J Dalle Ave, B.Sc. (University of Waterloo)

SUPERVISOR: Dr. Mark Inman

NUMBER OF PAGES: xiii, 99

ABSTRACT

Introduction

The airway epithelium, which acts as a protective barrier, is impaired in asthmatic patients and may contribute to abnormal airway function including hypersensitivity to inhaled particles. Chronic inflammation, a feature of asthma, is associated with structural changes in the airway epithelium including the transformation of columnar epithelial cells into mucin secreting goblet cells. Human epithelial cells exposed to Interleukin-13 (IL-13) *in vitro* resulted in goblet cell metaplasia and a significant drop in transepithelial resistance, indicating that barrier function is impaired.

Aim

We sought to determine whether goblet cell metaplasia alone is sufficient to impair airway epithelial barrier function *in vivo*.

Methods

Female BALB/c mice were infected with an adenovirus to overexpress IL-13, a control adenovirus, or no virus. Barrier integrity was assessed via single-photon emission computed tomography (SPECT) imaging by measuring the dispersion of technetium-labeled diethylene triamine pentaacetic acid (^{99m}Tc-DTPA) out of the lungs over time. Lung sections were stained by Periodic acid-Schiff to detect the presence of mucin-containing goblet cells.

Results

IL-13 exposure resulted in goblet cell metaplasia and associated airway hyperresponsiveness to methacholine. However, there was no significant increase in dispersion of ^{99m}Tc-DTPA over time from the airways in IL-13 overexpressed mice compared to control mice.

Conclusion

IL-13 induced goblet cell metaplasia did not impair the airway epithelial barrier to ^{99m}Tc-DTPA in our *in vivo* mouse model. We believe ^{99m}Tc-DTPA is a valid tool for assessing epithelial damage, as it has been used to quantify epithelial dysfunction in human asthmatics as well as animal models of asthma and animal models of epithelial disruption. Therefore, we conclude that epithelial dysfunction to DTPA observed in human asthmatics and in animal models of asthma are not due to IL-13 induced goblet cell metaplasia.

ACKNOWLEDGEMENTS

The McMaster faculty and students affiliated with the Firestone Institute for Respiratory Health have provided a comfortable and stimulating environment for me to work in. All of their support over the last couple of years is much appreciated. I would first and foremost like to thank my M.Sc. supervisor Dr. Mark Inman. He has been an excellent teacher and an inspiring researcher. I attribute much of my success to his guidance over the years.

I would also like to acknowledge the help of two of Dr. Inman's staff, Jennifer Wattie and Russ Ellis. Jennifer has worked with me on nearly all of my outcome days. Her willingness to help with my workload made my busy days in the lab much easier. Russ was very helpful training me how to work in a lab environment. I have become a better researcher with both of their support.

Outside of the lab environment I have been supported by my girlfriend, my friends, my brothers, and my entire family, and I am very thankful to them. I would especially like to thank my mom and dad for all their love and guidance over the years and for many more years to come. Thank you.

TABLE OF CONTENTS

ABSTRACT iii

ACKNOWLEDGEMENTS v

LIST OF FIGURES AND TABLES ix

LIST OF ABBREVIATIONS xi

CHAPTER 1: BACKGROUND 1

1.1 Introduction and Definition of Asthma 1

1.2 Epidemiology of Asthma 1

1.3 Clinical Manifestations and Treatment of Asthma 2

1.3.1 Forced Expiratory Volume in One Second and Forced Vital Capacity .. 2

1.3.2 Airway Hyperresponsiveness 4

1.3.3 Assessing Eosinophilic Inflammation 6

1.4 Immunology and Pathophysiology of Asthma 9

1.4.1 Allergen Sensitization 9

1.4.2 Subsequent Allergen Exposure and the Inflammatory Response 11

1.4.3 The Eosinophil 12

1.4.4 Interleukin-13 14

1.4.5 Structural Changes 16

1.5 Asthma Treatment 19

1.6 The Airway Epithelium 22

1.6.1 Function of the Airway Epithelium 22

1.6.2 The Airway Epithelium and Asthma 26

1.7 Goblet Cells 28

1.8 Gamma Aminobutyric Acid 30

1.8.1 Gamma Aminobutyric Acid Signalling 30
1.8.2 GABA in the airway epithelium 31
1.8.3 Goblet Cells and the GABAergic Pathway 33
1.9 Mouse Models of Asthma 34
CHAPTER 2: STUDY OUTLINE 38
2.1 Purpose of Thesis 38
2.2 Hypothesis 39
2.3 Study Design 39
CHAPTER 3: METHODOLOGY 45
3.1 Mice 45
3.2 Adenovirus Preparation and Delivery 45
3.3 Picrotoxin and Saline Control Preparation and Delivery 46
3.4 Lung Clearance Test to Assess Epithelial Permeability 46
3.5 Airway Responsiveness Measurements 47
3.6 Bronchoalveolar Lavage (BAL) 49
3.7 Lung Histology to Quantify Goblet Cells in the Airways 50
3.8 ELISA to Quantify IL-13 levels in the BAL Fluid 52
CHAPTER 4: RESULTS 54
4.1 Lung Clearance Test for Saline Groups 54
4.2 Lung Clearance Test for Picrotoxin Groups 58
4.3 Goblet Cells 64
4.4 Cell Differentials in the Bronchoalveolar Lavage (BAL) 67
4.5 Airway Responsiveness Measurements 69
4.6 IL-13 ELISA Results 73

CHAPTER 5: DISCUSSION 74
5.1 Summary of Purpose and Results 74
5.2 IL-13 Levels in the Bronchoalveolar Lavage (BAL) Fluid 75
5.3 Increased Goblet Cell Count in the Airways of Ad-IL-13 Mice 76
5.4 Airway Hyperresponsiveness in Ad-IL-13 Mice 79
5.5 IL-13 Overexpression Did Not Significantly Alter Airway Barrier Function 80
5.5.1 Summary of Lung Clearance Test 80
5.5.2 Differences Between In Vitro and In Vivo Models of Barrier Function . 81
5.5.3 The Role of Specific Tight Proteins 83
5.5.4 Relevency of the DTPA Lung Clearance Test 86
5.6 Conclusions 87
5.7 Future Directions 88
CHAPTER 6: REFERENCES 90

LIST OF FIGURES AND TABLES

Table Number	Title	Page Number
1	Experimental arms	43

Figure Number	Title	Page Number
1A	Representative SPECT imaging of ^{99m}Tc-DTPA dispersion out of the lung area over 20 minutes in ozone and room air exposed mice	41
1B	^{99m}Tc-DTPA clearance rate over time and area above the lung 99mTc-DTPA clearance curve over 20 minutes in air, ozone, and ozone + antioxidant treated mice	42
2	^{99m}Tc-DTPA dispersion in an Ad-IL-13 infected mouse and a control no virus mouse	55
3	^{99m}Tc-DTPA clearance over time in Ad-IL-13, Ad-dl-70, and no virus mice with daily saline treatment	56
4	Area above the lung ^{99m}Tc-DTPA clearance curve over 20 minutes in Ad-IL-13, Ad-dl-70, and no virus mice with daily saline treatment	57
5	^{99m}Tc-DTPA clearance over time in Ad-IL-13, Ad-dl-70, and no virus mice with daily picrotoxin treatment	60
6	Area above the lung ^{99m}Tc-DTPA clearance curve over 20 minutes in Ad-IL-13, Ad-dl-70, and no virus mice with daily picrotoxin treatment	61
7	^{99m}Tc-DTPA clearance over time in Ad-IL-13 + saline and Ad-IL-13 + picrotoxin treated mice	62
8	Area above the lung ^{99m}Tc-DTPA clearance curve over 20 minutes in Ad-IL-13 + saline and Ad-IL-13 + picrotoxin mice	63
9	Representative PAS stain of lung tissue section for all arms	65
10	Quantification of goblet cells	66
11	Total and Differential Inflammatory Cells in Bronchoalveolar Lavage Fluid	68

12	Airway resistance vs. nebulized methacholine dose response curve for saline treated mice	70
13	Airway resistance vs. nebulized methacholine dose response curve for picrotoxin treated mice	71
14	Airway resistance vs. nebulized methacholine dose response curve for adenovirus infected mice	72
15	IL-13 levels from the Bronchoalveolar Lavage fluid from saline treated groups	73

LIST OF ABBREVIATIONS

AHR	Airway Hyperresponsiveness
AMP	Adenosine Monophosphate
BAL	Bronchoalveolar Lavage
COPD	Chronic Obstructive Pulmonary Disease
CYS LT	Cysteinyl Leukotriene
DTPA	Diethylene Triamine Pentaacetic Acid
ECP	Eosinophil Cationic Protein
EDN	Eosinophil Derived Neurotoxin
EGFR	Epidermal Growth Factor Receptor
ELISA	Enzyme-Linked Immunosorbent Assay
EM	Electron Microscopy
eNO	Exhaled Nitric Oxide
EPO	Eosinophil Peroxidase
FeNO	Fraction of Exhaled Nitric Oxide
FEV_1	Forced Expiratory Volume in 1 Second
FVC	Forced Vital Capacity
GABA	Gamma Aminobutyric Acid
$GABA_AR$	Type A GABA Receptor
GAD	Glutamic Acid Decarboxylase
GM-CSF	Granulocyte-Macrophage Colony-Stimulating Factor

HDM	House Dust Mite
ICS	Inhaled Corticosteroids
IgE	Immunoglobulin E
IL	Interleukin
IN	Intranasal
INFγ	Interferon Gamma
IP	Intraperitoneal
IT	Intratracheal
JAK	Janus Kinase
LABA	Long Acting Beta Agonist
MARCKS	Myristoylated alanine-rich C-kinase substrate
MCh	Methacholine
MBP	Major Masic Protein
MHC	Major Histocompatibility Complex
NO	Nitric Oxide
NOS	Nitric Oxide Synthase
OVA	Ovalbumin
PBS	Phosphate Buffered Saline
PAF	Platelet-Activating Factor
PAS	Periodic acid-Schiff
PC_{20}	Provocative Concentration Causing a 20% Fall in FEV_1
PCR	Polymerase Chain Reaction

PLL	Poly-L-Lysine
R_{te}	Transepithelial Resistance
SABA	Short Acting Beta Agonist
SAL	Saline
SPECT	Single-Photon Emission Computed Tomography
STAT	Signal Transducer and Activator of Transcription
TC-DTPA	Technetium-Labelled Diethylene Triamine Pentaacetic Acid
TGFβ	Transforming Growth Factor Beta
Th2	Type 2 Helper T Lymphocyte
TNFα	Tumor Necrosis Factor Alpha
TSLP	Thymic Stromal Lymphopoietin
VCAM	Vascular Cell Adhesion Molecule
W-G	Wright Giemsa
ZO	Zonula Occluden

CHAPTER 1: BACKGROUND

1.1 Introduction and Definition of Asthma

Asthma is a respiratory disease characterized by variable airway obstruction and chronic inflammation. Derived from the Greek word for panting or noisy breathing, asthma can cause episodes of wheezing, shortness of breath (i.e. dyspnea), chest tightness, and coughing (Saunders, 1993; Lemanske and Busse, 2003). Airway obstruction occurs as a result of airway smooth muscle contraction with contributions from inflammation, edema, mucus secretion, and structural changes in the airway environment. This airway obstruction is often reversible either spontaneously or with treatment (Lemanske and Busse, 2003).

1.2 Epidemiology of Asthma

There are an estimated 300 million people worldwide who suffer from asthma, resulting in approximately 180 000 deaths each year (Masoli et al., 2004; Braman, 2006). Asthma incidences are currently increasing and are expected to reach a total of 400 million worldwide by the year 2025 (Masoli et al., 2004). Approximately one in ten North Americans and over 3 million people in Canada alone currently have asthma (Braman, 2006; Asthma Society of Canada, 2005). With approximately 2.2 million Canadian adults and 0.8 million Canadian children currently diagnosed with asthma, total estimated healthcare costs range between $504 million to $648 million each year in Canada (Kaplan et al., 2009). Asthma incidences are typically higher in westernized countries; however they

are currently rising in developing countries possibly due to increased urbanization as well as standardized definitions and treatment of asthma worldwide. Despite the increased prevalence of asthma in westernized countries there are proportionally less fatalities attributed to asthma exacerbations when compared to developing countries (Masoli et al., 2004). For example, based on data collected throughout the 1990s on patients between the ages of 5 to 34 years, Masoli et al. reported 1.6 deaths per 100 000 asthmatics in Canada versus 36.7 deaths per 100 000 asthmatics in China (Masoli et al., 2004).

1.3 Clinical Manifestations and Treatment of Asthma

1.3.1 Forced Expiratory Volume in One Second and Forced Vital Capacity

Measuring pulmonary function in asthmatic patients can help in assessing the severity of the disease as well as monitor the effectiveness of treatment. Spirometry is a physiological test that assesses how an individual inhales or exhales volumes of air as a function of time, which provides such outputs as the forced expiratory volume in one second (FEV_1) and the forced vital capacity (FVC) (Miller et al., 2005). Lung function measurements are often normal during remission; therefore emphasis is placed on the short-term variations in FEV_1 to help confirm the presence of uncontrolled asthma (Kaplan et al., 2009). Spirometry requires the patient to maximally inhale followed by exhaling with maximal forced expiratory effort, measuring the forced vital capacity (i.e. the maximum volume of air that can be exhaled) (Miller et al., 2005). FEV_1 is the

volume of air exhaled in the first second of a forced expiration from a position of full inspiration (Miller et al., 2005). To obtain a relative value that indicates an obstructive disease such as asthma versus a restrictive disease such as pulmonary fibrosis when FEV_1 is low, spirometry values are often presented as a ratio FEV_1 to FVC, which is usually greater than 0.80 in healthy Canadian adults (Bateman et al., 2008). To confirm reversibility of airflow obstruction in patients with a low FEV_1/FVC ratio and to help differentiate the condition from non-reversible obstructive diseases such as COPD, spirometry is performed again 15 – 20 minutes after administration of a fast acting bronchodilator (Kaplan et al., 2009). Asthma may be implied if FEV_1/FVC improves by more than 12% and at least 200 ml (Bateman et al., 2008).

A peak flow meter is another tool that can be used in patients suspected of having asthma. The fastest rate of expired airflow is measured by blowing as hard and as fast as possible into the peak flow meter after maximal inhalation (Kaplan et al., 2009). Variable changes in peak flow, usually compared in the morning and the evening, can imply asthma (Kaplan et al., 2009). A peak flow meter is easier to use, can be done at home, and can be used as a patient self-monitoring tool. However, peak flow meters do not measure flow rates over time or lung volumes, can have greater variation even among healthy individuals, and are less sensitive to changes in airway caliber compared to measuring FEV_1 (Kaplan et al., 2009).

1.3.2 Airway Hyperresponsiveness

Airway hyperresponsiveness (AHR), one of the characteristics of asthma, is defined as an increased ability of the airways to narrow after exposure to constrictor agents (O'Byrne and Inman, 2003). AHR consists of hypersensitivity and hyperreactivity in response to the constrictor agent or irritant. A patient who has hypersensitivity requires a smaller concentration of an irritant to initiate bronchoconstriction, while hyperreactivity is characterized by a greater increase in the magnitude of constriction in response to the irritant (O'Byrne and Inman, 2003). A methacholine (or any other airway constrictor agonist) challenge can be administered to measure airway responsiveness in patients suspected of having asthma, referred to as a bronchial provocation test. Methacholine acts directly on the muscarinic receptors of the airway smooth muscle, causing bronchoconstriction (Cockcroft and Davis, 2006). When plotted as a dose response curve, hypersensitivity is characterized by a shift of the curve to the left compared to healthy controls (i.e. bronchoconstriction occurs at a low dose of methacholine that would not measureably contract airway smooth muscle in a healthy airway) and hyperreactivity is demonstrated by greater maximal constriction. When percent change of FEV_1 is plotted vs. concentration of the constrictor agent, the slope of the line in a hyperresponsive individual is steeper compared to normal values, and there is no observed plateau effect (O'Byrne and Inman, 2003).

A bronchoprovocation test is a sensitive negative predictive test for asthma. Spirometry is performed after the patient inhales incremental doses of a smooth muscle agonist when baseline lung functions are normal (Lemanske and Busse, 2003). The provocative concentration (PC) 20 is defined as the concentration of an agonist causing a 20% fall in FEV_1 compared to baseline measurements. If the PC_{20} is at or above 16 mg/ml of methacholine in the absence of corticosteroid anti-inflammatory treatment, it is a strong indication that the patient under evaluation is unlikely to be asthmatic (Lemanske and Busse, 2003). A PC_{20} below 16 mg/ml could indicate asthma; however this is not appropriate to form a diagnosis as positive results may occur with allergic rhinitis, cystic fibrosis, and COPD (Kaplan et al., 2009).

Indirect stimuli can also be a trigger of AHR by initiating the release of mediators from inflammatory cells (Cockcroft and Davis, 2006). Common examples include exercise, hyperventilation of cold and dry air, and chemical stimuli such as adenosine monophosphate (AMP) and mannitol (O'Byrne and Inman, 2003; Cockcroft and Davis, 2006). These stimuli indirectly result in bronchoconstriction by increasing the osmolarity of the airways, triggering mast cell degranulation and a subsequent release of mediators that act on their receptors on the airway smooth muscle (Anderson, 2008). Bronchial provocation tests are also performed using these indirect stimuli in patients suspected of having asthma or when monitoring the effectiveness of treatment in asthmatics. An exercise challenge is a sensitive test that is usually performed while the

patient is running on a treadmill or riding a stationary bike; stimuli that a patient might encounter outside of a laboratory or clinical setting (unlike the inhalation of a direct smooth muscle agonist such as methacholine). FEV_1 or peak expiratory flow is measured before and after the exercise challenge. AMP can also be used in bronchial provocation tests because, like exercise, it triggers mast cell degranulation by increasing the osmolarity in the airways (Anderson, 2008). Similar to methacholine challenge, it is administered as an aerosol and nebulized to the patient; however, some studies have suggested a lack of comparability between results from the methacholine challenge and from an AMP challenge (Anderson, 2008). Possible explanations for these discrepancies include a large observed exhaled fraction of small particle AMP compared to methacholine (i.e. the AMP was not absorbed) as well as a difficulty in determining the equivalence of a dose of methacholine to a dose of AMP (Cohen et al., 2011). Mannitol is inhaled in increasing doses as a dry powder, and is sometimes preferred over exercise challenge because osmolarity of the airways is increased without the need to exercise to exertion (Anderson, 2008).

1.3.3 Assessing Eosinophilic Inflammation

Since a diagnosis of asthma often cannot be made from spirometry alone, assessing inflammation either directly or indirectly can be helpful to assess the airway environment. Eosinophilic inflammation, a feature of asthma, can be measured either directly with tools such as quantitative sputum cells counts or

indirectly by measuring exhaled nitric oxide. Assessing the level of eosinophilic inflammation can be useful to determine if the patient requires corticosteroid treatment and can also be used to monitor its effectiveness. Quantitative sputum cell count is a safe and well validated tool that differentiates between neutrophilic or eosinophilic inflammation in the airways (Hargreave, 2007). To induce sputum noninvasively and obtain secretions, the patient must inhale an aerosol of hypertonic saline promoting coughing and producing a sputum sample (Pizzichini et al., 2002). The concentration of saline is typically low, as it can induce bronchoconstriction in asthmatic patients, and some patients may be pretreated with a short acting bronchodilator (Pizzichini et al., 2002). The sputum is processed and stained to differentiate between inflammatory cells (Efthimiadis et al., 2002). Healthy non-asthmatics have an average of 0.4% eosinophils with a 90th percentile of about 1.1% eosinophils in the sputum (Brightling, 2006). Asthmatic patients have a wide scope of eosinophilic activity; ranging from a relative level similar to non-asthmatics to about 50% of the inflammation composed of eosinophils, as measured by induced sputum (Brightling, 2006). While this test may not identify all asthmatic patients due to some asthmatics having noneosinophilic asthma, it helps to identify patients who are targets for corticosteroid treatment, as corticosteroids characteristically suppress eosinophilic inflammation.

Nitric oxide (NO) is a gaseous signaling molecule that is produced by inflammatory cells such as eosinophils, endothelial cells in the bronchial

circulation, and airway epithelial cells throughout the respiratory tract in asthmatic patients (Baraldi et al., 2002). Exhaled NO (eNO) is measured as a biomarker of asthma reflecting underlying inflammatory activity (Barnes et al., 2010). Inflammatory cells and cytokines induce expression of the enzyme nitric oxide synthase (NOS) 2, which converts amino acids and generates NO (Barnes et al., 2010). NO is formed in the upper and lower respiratory tract and diffuses into the airway lumen where it mixes with the air that will be exhaled; however, some alveolar NO is taken up by hemoglobin (American Thoracic Society (ATS) and the European Respiratory Society (ERS), 2005). Levels of eNO can be affected by factors such as smoking, presence of an infection, and diet (Persson et al., 1994). When measuring eNO the adult patient inhales through a mouthpiece to total lung capacity and exhales over six seconds into a NO analyzer (ATS and ERS, 2005). If the fraction of exhaled nitric oxide (FeNO) is greater than 45 parts per billion the patient is likely to have high amounts of eosinophilic inflammation and is likely to respond well to corticosteroid treatment (Barnes et al., 2010). A low FeNO measurement of less than 25 parts per billion has a high predictive value for the absence of eosinophilic inflammation (Barnes et al., 2010). Therefore, measuring eNO is a noninvasive and reproducible test to indirectly measure eosinophilic inflammation when directly measuring eosinophils is not possible.

1.4 Immunology and Pathophysiology of Asthma

1.4.1 Allergen Sensitization

The development of asthma is likely due to a combination of hereditary and environmental factors rather than just environmental allergen exposure alone. A Danish study involving asthmatic twins has shown an increased prevalence of asthma in monozygous twins with identical genotypes compared to dizygous twins with an average of half of their genes in common (Skadhauge et al., 1999). Despite a presumed similar environment growing up, the monozygous twins had significantly higher rates of asthma compared to dizygous twins in this survey-based study (Skadhauge et al., 1999). Family studies have identified genes that are commonly present in asthmatic patients, such as the ADAM33 gene that is associated with airway hyperresponsiveness to inhaled methacholine, as an example (Meyers, 2011). The link between genetics and the development of asthma, genetics and the severity of the disease, as well as genes associated with asthma and their relationship between other respiratory diseases is still not well defined (Meyers, 2011).

Allergic sensitization contributing to asthma is the result of exposure to environmental allergens that generate antigen specific antibodies and elicit a type 2 helper T lymphocyte (Th2) response. Inhaled allergen peptides are taken up by antigen presenting cells, for example dendritic cells, macrophages, or B cells, located in the airway epithelium or submucosa via the major-

histocompatibility-complex (MHC) class II molecule and are displayed on the cell surface (Holgate, 2008). After allergen uptake, chemoattractants cause the antigen presenting cell to migrate to a draining lymph node to present the allergen to a naïve T lymphocytes (T cells) (Busse and Lemanske, 2001). T cells originate from stem cells in the bone marrow and undergo development in the thymus (Afshar et al., 2008). They migrate from the thymus as naïve T cells until they are stimulated to differentiate into effector T cells, helper T cells, or regulatory T cells (Afshar et al., 2008).

When allergic sensitization occurs the CD4 molecule on T cells binds preferentially to the MHC class II molecule which promotes differentiation into the Th2 type effector cell. Th2 cells activate B cells to promote antigen-specific immunoglobulin E (IgE) synthesis by two main mechanisms. Th2 cytokines such as interleukin-4 (IL-4) and IL-13 bind to B cells and activate the transcription factor signal transducer and activator of transcription (STAT) 6 (Busse and Lemanske, 2001). Additionally, B cells can bind to Th2 cells via the CD40 co-stimulatory protein (Bacharier et al., 1998). B cells then produce and release IgE which binds to mast cells in the airway or basophils in the peripheral blood via the high affinity IgE receptor FcεRI. Antigen specific memory T cells are also generated and reside in the airways to bind to their specific allergens, further driving the Th2 response (Afshar et al., 2008). Th2 cells also release IL-9 which attracts and plays a role in differentiation of mast cells in the airways (Barnes, 2008).

1.4.2 Subsequent Allergen Exposure and the Inflammatory Response

Mast cells are created in the bone marrow then migrate to the airways at the mucosal or submucosal surface where they fully mature (Galli, 1997). Once bound to IgE they play a critical role in the acute asthmatic response during subsequent allergen exposure, where they cross link with the antigen to release mediators stored in the cytoplasm contributing to bronchoconstriction and inflammation. Mast cells secrete histamine, prostaglandin D_2, and leukotriene C_4 which causes bronchoconstriction by acting on the H_1, DP_2, and $CysLT_1$ receptors respectively on the airway smooth muscle (Pelaia et al., 2008). Histamine is stored in granules, whereas prostaglandins, leukotrienes, as well as platelet-activating factor (PAF), which is also released from mast cells, are lipid mediators that are synthesized following mast cell activation to increase vascular permeability, increase mucus secretion, and contribute to the influx of inflammatory cells as part of the late phase asthmatic response (Barnes, 2008). Mast cells can also release the proteases tryptase, chymase, and carboxy-peptidase which act on protease activated receptors to contribute to the proinflammatory response (Bradding et al., 2006; Bradding et al., 2008). Additionally, mast cells synthesize and release proinflammatory cytokines including IL-4, IL-5, IL-13, granulocyte macrophage colony-stimulating factor (GM-CSF), and tumor necrosis factor alpha (TNF-α). These cytokines stimulate IgE synthesis from B cells, promote inflammation, and contribute to bronchial hyperresponsiveness. This immune response resulting in bronchoconstriction is

sometimes referred to as the early phase asthmatic response, which begins almost immediately after allergen exposure and usually resolves within an hour (Busse and Lemanske, 2001)

The late phase asthmatic response is characterized by an influx of inflammatory cells and the subsequent release of their mediators, which can develop four to six hours after the initial bronchoconstriction caused by allergen binding to IgE antibodies (Busse and Lemanske, 2001). Cytokines such as IL-3, IL-5, and GM-CSF activate eosinophils and chemokines such as those of the CC chemokine family (for example, CCL2, CCL, RANTES) to attract eosinophils to the airways and cause them to degranulate (Bloemen et al., 2007). Macrophages release PAF, reactive oxygen species, cytokines including IL-1, IL-6, interferon-gamma (INF-γ), TNF-α, and chemokines such as CCL2 and CCL3 (Bloemen et al., 2007). Some of these cytokines activate and attract neutrophils to the airways, increase mucus secretion and induce airway hyperresponsiveness to methacholine (Bloemen et al., 2007).

1.4.3 The Eosinophil

Named because its granules stain with eosin dye, eosinophils are one of the effector cells in asthma and may constitute a significant portion of the total number of inflammatory cells present in the disease. They are bone marrow derived inflammatory leukocytes that, in addition to their role in Th2 mediated asthma, are also present in the gastrointestinal tract and are activated in

response to parasitic infections. The eosinophil response in asthma has been extensively studied because it is not characteristically present in other chronic respiratory diseases.

Eosinophils are derived from pluripotent stem cells that express the cell surface molecule cluster differentiation 34 ($CD34^+$), and develop into eosinophils when simulated by IL-5, GM-CSF, or IL-13 (Rosenberg et al., 2007). IL-5 binds to the IL-5 receptor on eosinophils and their progenitors via the Janus kinase (JAK) signal transducer to activate transcription pathways and mature the eosinophil, resulting in its release into circulation (Rosenberg et al., 2007). IL-5 also promotes eosinophil survival in the peripheries. IL-5, IL-13, GM-CSF, and eotaxin promote eosinophil survival *in vitro*, and their absence in cell cultures significantly increases eosinophil apoptosis (Wegmann, 2011). Transgenic mouse models that were deficient in IL-5 or IL-5 receptor alpha (IL-5Rα) did not have an eosinophilic response when sensitized and challenged with ovalbumin (OVA); their eosinophil levels resembled unsensitized control mice (Foster et al., 1996). The IL-5 deficient mice did not show significant thickening of the basement membrane compared to wildtype and were not hyperresponsive to methacholine (Foster et al., 1996). Therefore, based on knockout mouse models of asthma, IL-5 was thought to be essential to drive eosinophilic inflammation resulting in AHR in asthma. However, targeting IL-5 in humans using the monoclonal antibody Mepolizumab did not eliminate asthma symptoms in clinical trials, despite reducing blood and sputum eosinophil levels (Wegmann, 2011).

IL-4, released by Th2 cells and mast cells, stimulates vascular endothelial cells and airway epithelial cells to produce chemokines that attract eosinophils to the airways (Rosenberg et al., 2007). IL-13 contributes to the influx of eosinophils in the airways by inducing the chemoattractant cytokine eotaxin in the airway epithelium (Rosenberg et al., 2007). IL-4 and IL-13 bind to the IL-4 receptor alpha on eosinophils to induce degranulation (Rosenberg et al., 2007). When they degranulate, eosinophils secrete proinflammatory cytokines and the cationic proteins eosinophil cationic protein (ECP), eosinophil peroxidase (EPO), major basic protein (MBP), and eosinophil derived neurotoxin (EDN) which can cause significant tissue damage, including airway epithelial damage (Rothenberg and Hogan, 2006). In addition to their cytotoxic properties, ECP and MBP have been associated with increased mast cell degranulation (Rothenberg and Hogan, 2006). Some eosinophil mediators also contribute to bronchoconstriction in asthma such as the lipid mediators leukotriene C_4 and PAF (Wegmann, 2011). Eosinophils may also play a role in the structural changes observed in asthma, as they release transforming growth factor β (TGF-β) which has been associated with fibrosis and collagen deposition in the airways.

1.4.4 Interleukin-13

First described in activated mouse Th2 cells, IL-13 acts on the alpha chain of the IL-4 receptor (type I IL-4 receptor and type II IL-4 receptor) as well as two IL-13 specific binding chains (IL-13Rα1 receptor and IL-13Rα2) (Hershey, 2003).

The IL-4 types I and II as well as the IL-13Rα1 receptor signaling is mediated by activation and phosphorylation of Janus tyrosine kinase and the transcription factor STAT6, which causes DNA transcription in the nucleus (Kuperman and Schleimer, 2008). Both IL-13 and IL-4, which are structurally similar, bind to type I and II IL-4 receptors; however, it is unclear why IL-13 produces different downstream effects compared to IL-4 (Hershey, 2003). IL-13Rα2 has been thought to be a decoy receptor due to a lack of any observed downstream signaling (Hershey, 2003). Recent publications have observed attenuated allergic responses when soluble IL-13Rα2 is administered in allergen challenge mice and have suggested that this receptor may be valuable for future therapeutic intervention studies (Andrews et al., 2009).

In addition to promoting eosinophil survival, activation, and recruitment, IL-13 acts on a variety of cell types contributing to allergic asthma; a few examples are briefly mentioned here. When IL-13 binds to the vascular endothelium it induces vascular cell adhesion molecule-1 (VCAM-1) which directs inflammatory cells such as eosinophils, T cells, monocytes, and basophils to the lung tissues (Bochner et al., 1995). B cell maturation and IgE production are increased in the presence of IL-13 originating from autocrine production from the B cells as well as from Th2 cells (Hajoui et al., 2004). IL-13 also acts on airway smooth muscle resulting in increased smooth muscle proliferation and increased contractile ability of smooth muscle cells *in vitro* (Hershey, 2003). When pretreated with IL-13 there was an increase in the maximum carbachol (a

cholinergic drug that induces smooth muscle contraction when it binds to the acetylcholine receptor) induced force generated in airway smooth muscle observed in tissue baths (Shore, 2004). IL-13 also increased the maximum force generated by histamine, acetylcholine, and leukotriene D_4 (Shore, 2004). This has translated to physiological effects observed in *in vivo* mouse models. Mice overexpressing IL-13 either by an inserted transgene or by adenoviral delivery display many of the observed features of asthma, including airway hyperresponsiveness to inhaled methacholine (Zhu et al., 1999). These mouse models of IL-13 overexpression also exhibit increased subepithelial fibrosis (Zhu et al., 1999). When bound to receptors on the airway epithelium IL-13 induces mucin production and subsequent mucus hypersecretion, induces goblet cell metaplasia, and decreases the beat frequency of ciliated epithelial cells (Laoukili et al., 2001).

1.4.5 Structural Changes

Structural changes in the airway environment have been observed in patients with asthma that are collectively referred to as airway remodeling. First described in 1922 by Huber and Koessler, asthma structural changes have been observed in large and small asthmatic airways (Bergeron et al., 2009). Subepithelial fibrosis, initially observed post mortem in cases of fatal asthma, has been measured throughout many levels of disease severity (Bergeron et al., 2009). Fibroblasts increase deposition of extracellular matrix proteins including

types I, III, and V collagen and fibronectin in the reticular lamina; the connective tissue just below the epithelial layer, as measured by electron microscopy (Elias et al., 1999). Subepithelial fibrosis has been linked with disease severity, a decline in FEV_1, and airway hyperresponsiveness to methacholine in human subjects (Boulet et al., 1997).

Airway smooth muscle area can increase with asthma; smooth muscle hypertrophy and hyperplasia has been observed in airways with increased disease severity (Kuwano et al., 1993). It is possible that the increased muscle area can result in a greater maximal contractile response, therefore contributing to airway hyperreactivity. It has also been suggested that the increased thickness of the airway wall could damage the lung parenchyma and therefore decrease their tethering forces, decreasing the resistance to any subsequent smooth muscle contractions (Elias et al., 1999). Analyses of autopsied lungs have found cartilage degradation in the large airways of asthmatics which could contribute to airway obstruction (Haraguchi et al., 1999). New blood vessel formation (angiogenesis) and increased size of the airway blood vessels have been reported in asthma, associated with greater expression of vascular endothelial growth factor (VEGF) (Li and Wilson, 1997).

Changes to the airway epithelium have also been observed in asthma, including epithelial shedding in bronchoalveolar lavage fluid and in biopsied tissue to a greater degree than healthy controls, loss of ciliated epithelial cells,

goblet cell hyperplasia, and upregulation of epidermal growth factor receptors including EGFR (Bergeron et al., 2009). The degree of epithelial damage has been correlated with airway hyperresponsiveness, which could imply a decreased ability to protect the internal airway environment from external irritants that can contribute to bronchoconstriction (Jeffery et al., 1989).

Structural changes were initially assumed to be a result of the inflammation present in asthmatic airways causing structural damage with a subsequent incomplete or inappropriate repair response. However, structural changes have been observed in early childhood asthma even before symptoms are present, suggesting at least some contribution to airway remodeling is inflammation independent (Warner and Knight, 2008). In a study examining atopic children without asthma, new blood vessel formation and increased vessel area was observed compared to non-atopic controls and to a similar extent of children already diagnosed with asthma (Barbato et al., 2006). While this study did not follow up to determine whether these children eventually were diagnosed with asthma, it demonstrated structural changes in the airways prior to symptoms of asthma. The authors speculated that the new blood vessels could provide new entry points for inflammatory cells into the airways and contribute to uncontrolled inflammation later in life (Barbato et al., 2006). In addition to this observed angiogenesis, atopic non-asthmatic children in this study also had increased thickness in the reticular basement membrane (Barbato et al., 2006). A recent study by Grainge et al. proposed that bronchoconstriction itself is the

cause of subepithelial collagen deposition in asthma (Grainge et al., 2011). They assigned asthmatic patients to one of four inhalation challenge protocols performed three times: methacholine, allergen, saline, or a short acting beta agonist plus methacholine (Grainge et al., 2011). Both the allergen and methacholine group achieved bronchoconstriction and the allergen group also exhibited subsequent inflammation (Grainge et al., 2011). Interestingly, both the allergen and methacholine groups had significantly increased levels of subepithelial collagen band thickness and goblet cell hyperplasia compared to the control groups, despite all patients being asthmatic. There was no significant difference between the allergen and methacholine groups; therefore the bronchoconstriction without additional inflammation was sufficient to increase subepithelial collagen deposition (Grange et al., 2011).

1.5 Asthma Treatment

Although there is not one standardized treatment for asthma, there are many pharmacological agents available to asthmatic patients that have demonstrated some level of efficacy in managing symptoms. Inhaled beta-2 (β_2)-agonists are bronchodilators that bind to the β_2-adrenergic receptor on the airway smooth muscle resulting in muscle relaxation. There are two types of inhaled β_2-agonists available for asthmatics patients: short acting (SABA) and long acting (LABA). SABAs such as salbutamol have demonstrated partial prevention of smooth muscle contraction when taken before allergen challenge or exercise and

can partially reverse the late asthmatic response (O'Byrne, 2009). However, SABAs do not decrease the inflammation in the airways nor are they effective as regular treatment for controlling asthma because they can cause tolerance to their protective effects on bronchoconstriction (Cockcroft et al., 1993). LABAs such as salmeterol have a slower onset of action compared to SABAs, but last about 12 hours (vs. 4-6 hours for SABAs). LABAs have been shown to be less effective than inhaled corticosteroids (ICS) in terms of controlling symptoms and reducing exacerbations, and are often given in combination with ICS therapy to reduce the amount of steroids taken by the patient (Rees, 2006). Other bronchodilators such as tiotropium bromide, an anticholinergic drug commonly prescribed to COPD patients, have also improved symptoms and lung function when combined with ICS (Peters et al., 2010).

Regular treatment with ICS has been among the most effective strategies for controlling asthma and reducing inflammation in both the early and late phases of the asthmatic response (O'Byrne, 2009). Corticosteroids induce eosinophil apoptosis and inhibit the response to proinflammatory cytokines such as interleukin-5 and granulocyte-macrophage colony stimulating factor (Wegmann, 2011). Regular treatment with ICS improves pulmonary function and reduces exacerbations and fatalities associated with asthma.

Leukotriene inhibitors such as montelukast can also be used to manage asthma symptoms either by inhibiting production of the enzyme 5-lipoxygenase

which is involved in cysteinyl leukotriene production or by blocking the cysteinyl leukotriene receptor Cys LT_1 on the airway smooth muscle (O'Byrne, 2009). Leukotriene inhibitors have shown to attenuate the early asthmatic response, and to a lesser degree the late asthmatic response, as well as decrease allergen induced airway eosinophilia (Leigh et al., 2002). Histamine antagonists such as desloratadine, also referred to as antihistamines, block the H_1 receptor on the airway smooth muscle which has shown to moderately attenuate bronchoconstriction in the early but not the late asthmatic response (O'Byrne, 2009). When a single dose of histamine antagonist is taken in combination with a leukotriene inhibitor prior to allergen challenge, a significant decrease in the late asthmatic response and eosinophil recruitment into the lungs has been observed (Davis et al., 2009).

The anti-IgE monoclonal antibody omalizumab is also given to patients with asthma, often if it is uncontrolled with ICS alone. Omalizumab binds to circulating IgE, preventing them from binding to mast cells or other effector cells (Bang and Plosker, 2004). Omalizumab alone has not managed asthma symptoms as well as ICS, but can be used in combination or to decrease the ICS dose (Bang and Plosker, 2004). Another monoclonal antibody for asthma treatment is mepolizumab, an anti-IL-5 drug which has been shown to significantly decrease airway and blood eosinophils by binding to IL-5 in early clinical trials (Busse et al., 2010).

1.6 The Airway Epithelium

1.6.1 Function of the Airway Epithelium

The bronchial epithelium consists of ciliated cuboidal cells, non-ciliated surfactant-secreting Clara cells, mucus-secreting goblet cells, and basal cells (Holgate, 2007; Davis and Dickey, 2008). In healthy individuals it forms a physical barrier to keep out harmful inhaled particles and is complemented by mucociliary clearance, where the cilia that project into the lumen beat in waves to remove mucus and trapped particles towards the esophagus until it is swallowed (Rogers, 2003). The effectiveness of the epithelium to keep out inhaled particles is partially dependent on tight junctions; proteins located primarily at the apical side of epithelial cells that selectively allow passage of material across the epithelial layer (Godfrey, 1997; Holgate, 2007). Epithelial cell plasma membranes have relatively low permeability, therefore molecules crossing the barrier will move between epithelial cells rather than through them (Claude and Goodenough, 1973). The epithelial tight junctions, also called zonulae occludens, regulate the passage of water, ions, and inflammatory cells through the fluid filled spaces between epithelial cells (Godfrey, 1997). Tight junctions allow the diffusion of selective inorganic ions; however, they prevent macromolecules from diffusing through the barrier even at low levels of electrical resistance (Gumbiner, 1987). Interestingly, polymorphonuclear leukocytes (i.e. granulocytes) induce paracellular permeability resulting in their transmigration

across the epithelium, although the mechanism of this selective transport is not understood (Nash et al., 1988). More recent studies examining the transmigration of neutrophils across the epithelial layer in the intestines contributing to inflammatory bowel disease have suggested that the inflammatory mediators may down regulate specific tight junction proteins allowing for the passage of inflammatory cells (Kucharzik et al., 2001).

Tight junctions consist of transmembrane proteins and anchoring junctions that bind them to the cytoskeleton of the epithelial cell (Godfrey, 1997; Holgate, 2007). They were first described in 1963 by Farquhar and Palade, who first observed them in various organs by electron microscopy and proposed the term zonulae occluden (Farquhar and Palade, 1963; Godfrey, 1997). To investigate their role as a barrier, Farquhar and Palade administered different electron dense tracer molecules in rats intraperitoneally and examined the epithelial tissue from various organs *ex vivo* (Farquhar and Palade, 1963). They were able to follow the dense mass of the tracer down to the levels of the epithelial tight junctions and found none of the tracer beyond that point without any evidence of a concentration gradient down the junctional complex (Farquhar and Palade, 1963).

In 1973, Claude and Goodenough observed epithelial cells from various animal tissues *in vitro* and labeled them “very leaky, leaky, intermediate, tight, and very tight” based on measurements of transepithelial resistance (i.e. the

movement of ions across the epithelium, measured in ohms per square centimeter, $\Omega\ cm^{-2}$) (Claude and Goodenough, 1973). They not only reported that transepithelial resistance varied between the epithelia of different organs, but also that tight epithelia (i.e. with a high transepithelial resistance) were associated with more zonnulae occludentes; junctions with more strands were found to be “tighter” than junctions with less strands of tight junction proteins, based on freeze-fracture electron microscopy images (Claude and Goodenough, 1973).

Comparisons of tight junction images in airway epithelial cells have been made between different cell types. Using freeze-fracture electron microscopy, Matsumura and Setoguti imaged the junctions between adjacent ciliated cells and goblet cells in normal human bronchial epithelium (Matsumura and Setoguti, 1989). They reported a large number of connecting strands between two adjacent ciliated epithelial cells (7 – 11 nearly parallel strands), but only a small number of strands (2 – 4) between adjacent goblet cells (Matsumura and Setoguti, 1989). They did not perform any functional experiments to compare the effectiveness of the junctions between these two cells types as a passive barrier. In a more recent study, Lachowicz-Scroggins et al. measured the transepithelial resistance of human epithelial cells *in vitro*, compared with the transepithelial resistance in human epithelial cells from the same cultures that were exposed to IL-13 to induce goblet cell metaplasia (Lachowicz-Scroggins et al., 2010). The strips of human epithelium were exposed to 10 ng/ml of recombinant human IL-

13 for seven days (Lachowicz-Scroggins et al., 2010). Mucin content as measured by enzyme-linked immunosorbent assay (ELISA) was significantly elevated in the IL-13 treated group, with the highest levels measured on the final day of the 7 day IL-13 exposure protocol (Lachowicz-Scroggins et al., 2010). The total number of goblet cells significantly increased from an average of 352 goblet cells in the control group to an average of 674 goblet cells in the IL-13 treated group, as detected by the antibody B6E8 (an antibody specific for human airway goblet cells) in a field of 320 x 320 μm (Lachowicz-Scroggins et al., 2010). IL-13 did not cause a significant change in the total number of cells compared to the control group; however, there was a significant decrease in the transepithelial resistance (R_{te}) in IL-13 treated epithelial cells compared to control (R_{te} of 1 536 ± 93 Ω cm^2 in control vs. R_{te} of 966 ± 86 Ω cm^2 in IL-13 treated group) (Lachowicz-Scroggins et al., 2010). Therefore, based on these results, IL-13 mediated goblet cell metaplasia resulted in a decreased transepithelial resistance compared to the control group.

In addition to acting as a physical barrier to protect the internal environment, the airway epithelium plays a role in the immune response and immune regulation. It is capable of releasing multiple cytokines that contribute to the asthmatic response including IL-6, IL-8, GM-CSF, and thymic stromal lymphopoietin (TSLP) when stimulated with certain proinflammatory cytokines and in response to certain respiratory viruses (Proud and Leigh, 2011). IL-6 is capable of inducing IgE synthesis from B cells and contributes to the

differentiation of naïve T cells into Th2 cells (Cromwell et al., 1992). IL-8 attracts and activates neutrophils in the airway environment (Leonard and Yoshimura, 1990). TSLP is an IL-7-like cytokine (it shares a similar genetic structure and acts on the IL-7Rα chain) derived from epithelial cells that is sufficient to activate human dendritic cells and maintain their survival in cell cultures (Soumelis et al., 2002). Soumelis et al. further demonstrated that the TSLP-activated dendritic cells induced a greater Th2 proliferative response when exposed to naïve T cells compared to IL-7-activated dendritic cells or lipopolysaccharide-activated dendritic cells *in vivo*, which could imply it contributes to the sensitization to allergens (Soumelis et al., 2002). TSLP can induce Th2-attracting cytokines such as CCL17 at the airway epithelium (Ying et al., 2005). TSLP expression has been correlated with FEV_1 in severe asthmatics (Ying e al., 2005).

1.6.2 The Airway Epithelium and Asthma

In asthmatic airways there is evidence of an impaired (leaky) epithelial barrier function. Bronchial epithelial cell shedding has been observed based on sputum samples and bronchial biopsies of asthmatic patients, where the degree of epithelial shedding has been correlated with the patients' airway hyperresponsiveness to methacholine (Montefort et al., 1992).

A lung clearance test can be performed to give an index of airway barrier function *in vivo* by measuring the dispersion of an inhaled marker out of the airways (Godfrey et al., 1997). Bhure et al. nebulized diethylene triamine penta-

acetate (DTPA), a low molecular weight marker commonly used in lung clearance tests, as a non-invasive evaluation of epithelial permeability (Bhure et al., 2009). The DTPA was bound to technetium-99m, a metastable nuclear isomer generated to have a longer half-life than technetium-99, which is used as a radio label to track dispersion of the DTPA out of the airways using a gamma camera (Bhure et al., 2009). Bhure et al. performed lung clearance test on a group of non-smoking healthy volunteers as well as 15 non-smokers diagnosed with chronic persistent asthma (Bhure et al., 2009). Asthmatic patients were free to take their prescribed medication as directed, and were clinically stable at the time of the lung clearance test. Technetium-99m labeled DTPA (^{99m}Tc-DTPA) was nebulized using a dry aerosol chamber attached to a face mask for inhalation, where participants inhaled at normal tidal volume while lying supine on a gamma camera table (Bhure et al., 2009). Baseline data was presented as $T_{1/2}$; the time required for 50% of the ^{99m}Tc-DTPA to disperse out of the pre-defined region of interest, in this case the area over each lung (Bhure et al., 2009). The asthmatic group had a $T_{1/2}$ of 24.06 ± 6.19, significantly smaller than the control group which had a $T_{1/2}$ of 50.95 ± 16.58 minutes (Bhure et al., 2009). Therefore, based on a lung clearance test *in vivo* using nebulized ^{99m}Tc-DTPA, the asthmatic group had increased epithelial permeability in the airways (Bhure et al., 2009). Although the lung clearance test does not measure epithelial permeability directly, it is a sensitive and reproducible test where the integrity of epithelial tight junctions are regarded to be the rate limiting step (Godfrey, 1997).

Damage to the respiratory epithelium stimulates the epidermal growth factor (EGF) cascade at the site of injury (Rogers, 2003; Gardner et al., 2010). EGF and the EGF receptor (EGFR) stimulate proliferation and migration of lung epithelial cells to restore lung epithelial integrity (Crosby and Waters, 2010). *In vitro* studies using murine bronchial epithelial cells have shown that increased levels of transforming growth factor alpha (TGF-α) will stimulate epithelial repair similar to the observed effects of EGFR signaling (Crosby and Waters, 2010). EGFR activity is increased in asthmatic patients compared to non-asthmatics, and appears to increase with disease severity (Crosby and Waters, 2010; Davies, 2001). Interestingly, a study by Allahverdian and colleagues has shown that IL-13 produced by cultured human epithelial cells in response to mechanical injury increases EGFR activity and enhances epithelial repair (Allahverdian et al., 2008). However, despite an increased level of EGFR activity the airway epithelium remains leaky in some asthmatics suggesting an incomplete epithelial repair (Davies, 2001). Allahverdian and colleagues have suggested that perhaps prolonged release of IL-13 in asthma would have adverse effects on epithelial and subepithelial structures that would not be detected in an acute model of mechanical epithelial injury (Allahverdian et al., 2008).

1.7 Goblet Cells

Goblet cells are columnar epithelial cells that secrete mucus which traps inhaled particles, bacteria, and viruses, and maintains hydration in the airways

(Voynow and Rubin, 2009). The mucus, along with any particles that are trapped, is continually cleared from the airways by ciliary beat activity. To further aid in protecting the body from microorganisms, mucus has antioxidant, antiprotease, and antimicrobial activity (Voynow and Rubin, 2009).

Mucus is an aqueous solution that contains mainly mucins; high molecular weight glycoproteins that are released from secretory granules inside the goblet cells (Lu and Inman, 2009; Rogers, 2003). There are many genes in the MUC family that produce mucin proteins including MUC5AC and MUC5B, which are most commonly associated with the mucus secreted in the airways (Rogers, 2003). Mucin is released into the surface of the airways via the phosphorylation of the enzyme alanine-rich C kinase substrate (MARCKS), releasing the mucin granule from the apical surface of the cell (Davis and Dickey, 2008). Once released from their granules mucins expand and become hydrated, forming a layer of mucus (Rogers, 2003). Dephosphorylation of MARCKS causes it to hold on to the mucin granule preventing further mucin secretion (Rogers, 2003).

Mucus overproduction and goblet cell hyperplasia are features of asthma. Goblet cells increase in number and in size in asthmatic patients and begin to appear in the small airways where they are normally absent (Rogers, 2003). In the larger airways the increased mucus buildup can be dislodged by cough; however, hypersecretion in the small airways can compromise mucociliary clearance resulting in mucus trapping contributing to airflow obstruction (Rogers,

2003). The goblet cell hyperplasia and metaplasia in the airways is associated with the Th2 allergic response. The Th2 cytokine IL-13 is sufficient to induce goblet cell metaplasia resulting in mucus overproduction based on transgenic overexpression models (Zhu et al., 1999).

1.8 Gamma Aminobutyric Acid

1.8.1 Gamma Aminobutyric Acid Signalling

Gamma Aminobutyric Acid (GABA) is a neurotransmitter in the central nervous system which acts at inhibitory synapses by binding to transmembrane receptors in the plasma membrane of pre-and postsynaptic neuronal processes (Lu and Inman, 2009). GABA facilitates inhibition by allowing negatively charged chloride ions to enter the cell or positively charged potassium ions to leave the cell causing hyperpolarization (Lu and Inman, 2009).

GABA is synthesized from the amino acid glutamate, also called glutamic acid, by the enzyme glutamic acid decarboxylase (GAD) (Erlander et al., 1991). There are two forms of GAD: GAD65 and GAD67 (Erlander et al., 1992). GAD65 is anchored to synaptic vesicles in axon terminals and releases GABA to the extracellular space by exocytosis, while GAD67 is free in the cytosol (Vinkers et al., 2010). Once released from the cell GABA acts on two cell surface receptors: the subtype A GABA receptor ($GABA_AR$) and the subtype B GABA receptor ($GABA_BR$) (Erlader et al., 1991). The $GABA_AR$ contains five subunits to form a ligand gated chloride channel, consisting of different combinations of 19 possible

subunits (Vinkers et al., 2010). When GABA binds to the $GABA_AR$ the flow of negatively charged chloride ions entering the neuron increases, causing hyperpolarization and an inhibitory postsynaptic signal (Vinkers et al., 2010). Different pharmacological agents can bind to the $GABA_AR$ depending on the subunits present; however, $GABA_AR$ mediated anionic conductance can be blocked by bicuculline, a competitive receptor antagonist, or picrotoxin, a noncompetitive channel blocker (Lu and Inman, 2009). The $GABA_BR$ is a G protein coupled receptor that stimulates potassium channels in the neuron (Lu and Inman, 2009).

1.8.2 GABA in the airway epithelium

While the role of GABA in the central nervous system had been studied for some time, GABA had not been extensively examined in the lung environment until messenger ribonucleic acid (mRNA) for a $GABA_AR$ subtype had been detected in the lung in the late 1990's by Hedblom and Kirkness (1997). Using polymerase chain reaction (PCR) to detect $GABA_AR$ mRNA in various human and rat tissues outside of the central nervous system, Hedblom and Kirkness reported finding "enriched" levels of $GABA_AR$ in lung, thymus, prostate, and uterus tissue (Hedblom and Kirkness, 1997). The $GABA_AR$ subunit found in these tissues, termed the pi (π) subunit or GABRP, is abundant in these peripheral tissues but rarely detected in the brain (Jin et al., 2005).

In 2004 the Liu lab based out of Oklahoma State University published a paper examining biomarkers for type I and type II alveolar epithelial cells (Chen et al., 2004). Using real-time PCR Chen et al. found deoxyribonucleic acid (DNA) expression of GABRP in type II alveolar epithelial cells (cuboidal cells that synthesize and secrete surfactant) taken from rat lungs, and confirmed these findings with in situ hybridization (Chen et al., 2004). GABRP was not found in type I alveolar epithelial cells (squamous alveolar cells responsible for gas exchange) (Chen et al., 2004). Using immunohistochemistry they were able to stain GABRP in type II alveolar epithelial cells and in bronchial epithelial cells (Chen et al., 2004).

In 2007 the Lu lab based out of the University of Toronto published a paper to confirm the presence of $GABA_AR$ in airway epithelial cells and to determine whether GABAergic signaling had any role in airway physiology (Xiang et al., 2007). Using immunoblot assays they reported expression of GAD65, GAD67, and various subtypes of $GABA_AR$ in human type II alveolar epithelial cells, human small airway epithelial cells, human bronchial epithelial cells, and mouse lung tissues, suggesting there is GABAergic signaling in airway epithelial cells (Xiang et al., 2007). Using lung tissues from naïve mice they performed immunoflorescence staining and observed that GAD65 and GAD67 was present in all bronchial epithelial cells and in some of the alveolar epithelial cells (Xiang et al., 2007).

1.8.3 Goblet Cells and the GABAergic Pathway

When treating human small airway epithelial cells with GABA Xiang and colleagues observed greater mucin glycoproteins as stained by alcian blue, which implies a role for GABA in mucus production in the epithelium (Xiang et al., 2007). To determine whether GABA signaling affects mucus secretion in asthma, female BALB/c mice (6-8 weeks old) were sensitized and challenged with ovalbumin (OVA) to model the effects of allergic asthma (Xiang et al., 2007). Twenty-four hours after OVA challenge the mice had significantly increased expression of GAD65, GAD67, and $GABA_AR$ (Xiang et al., 2007). This trend was also observed in human tissues twenty-four hours after allergen inhalation challenge (Xiang et al., 2007). Cell cultures of human small airway epithelial cells treated with the Th2 cytokine IL-13 exhibited increased expression of GAD65, GAD67, and $GABA_AR$ (Xiang et al., 2007). 0.5μg of recombinant IL-13 was given intranasally (i.n.) to female BALB/c mice which also increased GAD65, GAD67, and $GABA_AR$.

Xiang and colleagues also determined that IL-13 is the necessary factor in the Th2 allergic response that increases GABA signaling in the airway epithelial cells in an IL-13 knockout model (Xiang et al., 2007). Mice lacking the IL-13 gene that were sensitized and challenged to OVA did not increase expression of GAD65, GAD67, or $GABA_AR$ (Xiang et al., 2007). Goblet cell numbers or mucus levels were not reported.

Goblet cells arise by differentiation of airway epithelial cells rather than by division of other goblet cells (Rogers, 2003). Allergen exposure in sensitized individuals and the subsequent Th2 mediated allergic response triggers goblet cell metaplasia and mucus overproduction contributing to airway obstruction. Based on their *in vivo* OVA, recombinant i.n. IL-13, and IL-13 deficient mouse models, Xiang et al. concluded that this goblet cell differentiation is mediated by the GABAergic signaling in airway epithelial cells (Xiang et al., 2007). IL-13 given either directly or indirectly as a result of allergen exposure in sensitized mice activate the GAD 65 and GAD67 enzymes to produce GABA from glutamate, which acts on the $GABA_AR$ to transform airway epithelial cells into goblet cells (Lu and Inman, 2009). The $GABA_AR$ blockers picrotoxin or bicuculline given i.n. or intraperitoneally (i.p.) greatly suppressed the increase in goblet cells and mucus overproduction *in vivo* in the mouse models of OVA sensitization and with recombinant i.n. IL-13 exposure compared to control groups (Xiang et al., 2007). Blocking the $GABA_AR$ with picrotoxin or bicuculline did not prevent increased levels of IL-13 in the bronchoalveolar lavage (BAL) fluid in the OVA model nor did it prevent an inflammatory response or AHR to methacholine in the OVA or i.n. IL-13 model (Xiang et al., 2007).

1.9 Mouse Models of Asthma

Animal models of asthma have been used extensively and influence what we currently understand about the disease. While animal models allow us to

manipulate some of the variables of asthma, it is important to keep in mind the limitations of animal models, a few of which are highlighted here. Asthma conditions must be induced in mice as they do not spontaneously develop asthma that resembles the condition in humans. Given that asthma is a complex disease with variable clinical characteristics involving multiple mechanisms, reproducing it in its entirety in mice may be impossible (Bates et al., 2009). There are a wide variety of mouse models used including inducing a Th2 response using a variety of antigens and various routes of administration, models of cellular adoptive transfer, gene overexpression, and transgenic knockout models (Epstein, 2004). However, different strains of mouse (for example, BALB/c, A/J, C3H/HeJ, or C57BL/6) react differently to the same experimental conditions, implying genetic factors pay a role in the manifestation of asthma (Shinagawa and Kojima, 2003). For example, the A/J strain of mouse develops airway hyperresponsiveness shortly after allergen challenge to a much greater degree than other strains of mice (Bates et al., 2009). Different strains of mouse display different levels of airway remodeling in chronic allergen protocols (Shinagawa and Kojima, 2003). Therefore, both the strain of mouse and the protocol used for allergen sensitization can affect the development of asthma like conditions in mice, limiting the ability to generalize findings to other mouse strains and also to humans. Other limitations of the mouse model of asthma include the lack of any observed late phase asthmatic response to inhaled allergens (Epstein, 2004). Mice demonstrate smaller shifts in airway sensitivity

after allergen challenge compared to humans and in some models the AHR does not persist, unlike human asthma that typically displays persistent AHR even during remission. The inflammatory response in mouse models of allergic asthma also does not perfectly mirror that seen in human asthma, as eosinophil degranulation in mice has not been convincingly demonstrated by transmission electron microscopy (Malm-Erjefält et al., 2001). Eosinophil mediators such as EPO have not been detected in the lung environment, and were found to be retained in the cell in *in vitro* studies (Malm-Erjefält et al., 2001). Therefore, mouse models of allergic asthma can be useful to observe the migration of eosinophils, but not to observe the consequences of eosinophil mediator release.

Animal models of allergic asthma reproduce many features of the disease and can be used by researchers as a tool to study conditions as similar to those observed in human patients as possible. However, a model reproducing just one feature of asthma can also be useful depending on the research question being studied as it allows researchers to observe the effects of one manipulated variable at a time, further understanding its role in the disease. Adenoviral mediated gene transfer is one tool available to understand the role of a specific cytokine in an *in vivo* animal model. It is used in animal research to overexpress a desired cytokine and can be advantageous over transgenic models if it is preferred that the animal mature into adulthood under similar conditions as control animals. When infected into a host animal, the encoded cytokine gene is produced from infected cells (Ramshaw et al., 1992). While this tool allows for

investigating of the *in vivo* function of a cytokine, it is important to remember that it does not completely mimic the *in vivo* conditions under which it would be produced locally (Xing et al., 1994). Therefore, high amounts of a particular cytokine can be produced *in vivo*, allowing researchers to study its effects in an animal model. Cytokine production will continue for a short duration, reaching a peak at 7 days post infection, before the host immune response will begin to clear the virus (Sime et al., 1997). It is important to keep in mind that the host animal will mount an immune response to the virus; therefore not all inflammatory changes can be attributed to the overexpression of the cytokine alone.

CHAPTER 2: STUDY OUTLINE

2.1 Purpose of Thesis

Epithelial damage is a feature of asthma, but the cause and the consequences of an impaired epithelial barrier are poorly understood. Damaged or decreased tight junction proteins that span across two adjacent epithelial cells have resulted in a decreased transepithelial resistance *in vitro* and an increased dispersion of a radio-labeled aerosol out of the airways *in vivo* (Holgate, 2007; Ilowite et al., 1989).

Structural and functional changes occur in asthmatic airways such as goblet cell metaplasia and, subsequently, mucus overproduction. Electron microscopy imaging has shown that there are less tight junction strands between adjacent goblet cells in the epithelium compared to adjacent ciliated columnar epithelial cells (Matsumura and Setoguti, 1989). Since tight junction strands are believed to be necessary to form a tight epithelium, and there are less tight junction strands between goblet cells, it is possible that the transformation of columnar epithelial cells into goblet cells (i.e. goblet cell metaplasia) that occurs in asthmatic airways results in the impaired, or leaky, barrier function.

The purpose of this study is to evaluate the contribution of goblet cell metaplasia to the impaired epithelial barrier function observed in asthmatic patients. We will use a mouse model to induce goblet cell metaplasia in the

airways and measure the permeability of the epithelium to a radio-labeled aerosol *in vivo*.

2.2 Hypothesis

Goblet cell metaplasia contributes to the impaired barrier function observed in asthma. In this study, goblet cell metaplasia will result in impaired epithelial barrier function in female BALB/c mice. There will be a significant increase in the dispersion of radio-labeled aerosol out of the airways in mice with goblet cell hyperplasia compared to control.

2.3 Study Design

We induced goblet cell metaplasia in mouse airways by administering the cytokine IL-13 on an adenoviral vector (Ad-IL-13). Previous studies have shown that when an adenovirus is administered intratracheally the vectors infect the respiratory epithelium and produce the inserted gene products that are functionally active, in this case the overexpression of IL-13 to induce goblet cell metaplasia (Xing et al., 1994). Therefore, IL-13 will be produced locally within the affected tissue at high concentrations (Xing et al., 1994). Peak expression of adenovector-mediated gene transfer in the epithelium occurs seven days after infection and declines by day fourteen (Sime et al., 1997). We chose to perform outcomes measurements 10 days after administering the adenovirus.

Our primary outcome, epithelial barrier function, was assessed by measuring the dispersion of a radio-labeled aerosol over time. We instilled the aerosol diethylene triamine penta-acetate (DTPA) bound to technetium-99m (^{99m}Tc-DTPA), as this has been used in the literature in clinical settings and previously in our lab in mouse models of asthma (see **Figure 1** for an example of lung ^{99m}Tc-DTPA clearance data from a previous study performed in our lab which can serve as a positive control for airway epithelial barrier dysfunction). Using a single-photon emission computed tomography (SPECT) machine for small animals we tracked ^{99m}Tc-DTPA dispersion for 20 minutes. In our previous models of barrier dysfunction in female BALB/c mice, we were able to detect a significant difference in the dispersion of DTPA out of the airways 20 minutes after administration compared to control groups.

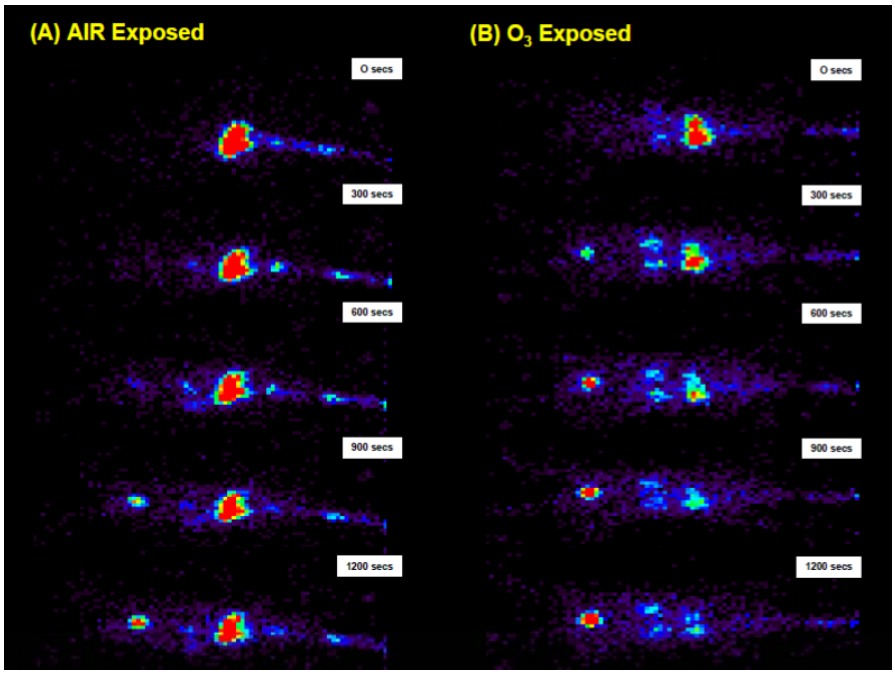

Figure 1A: Representative SPECT imaging of ^{99m}Tc-DTPA dispersion out of the lung area over 20 minutes

This image from Frank DiGiovanni's 2009 thesis (unpublished data) on ozone (O_3) exposure and airway barrier dysfunction. The room air exposed mouse (left) has most of the radio-labeled aerosol remaining in the lungs after 20 minutes, as indicated by the dark red area of radioactivity. The O_3 exposed mouse (right) does not have as high of a concentration in the lung area; most of the radiation has dispersed throughout the body. Increased ^{99m}Tc-DTPA dispersion is attributed to increased epithelial permeability compared to the room air exposed mouse. This trend of ^{99m}Tc-DTPA dispersion attributed to a leaky epithelium compared to control has been reproduced in our lab in a model of eosinophil degranulation (Ariel Hendin, unpublished thesis 2010) and poly-L-lysine administration (Jodie Powdrill, unpublished thesis 2009). These results can serve as a positive control of a damaged airway epithelium. We expect our control groups to mirror the air exposed mice represented on the left, and our group of mice with increased goblet cells to mirror the dispersion represented on the right.

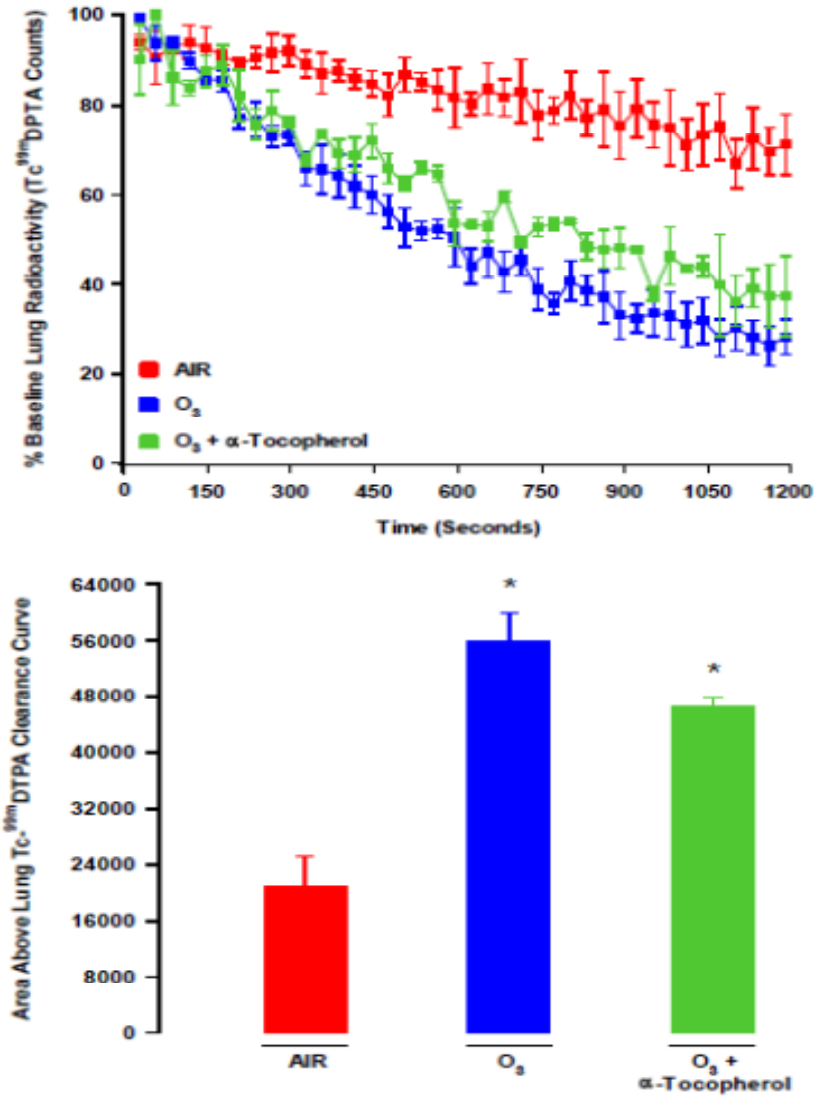

Figure 1B: ^{99m}Tc-DTPA clearance rate over time (top) and area above the lung ^{99m}Tc-DTPA clearance curve over 20 minutes in air, ozone, and ozone + antioxidant treated mice

These images from DiGiovanni's ozone study quantify the dispersion of ^{99m}Tc-DTPA out of the lung area. After 20 minutes, the ozone exposed mice had a significant increase in the dispersion of ^{99m}Tc-DTPA from baseline compared to control (room air exposed mice). We expect goblet cell metaplasia to result in a similar rate of ^{99m}Tc-DTPA clearance from the lung area in our study.

To assess the changes in barrier function and to be able to attribute the changes to the goblet cell metaplasia, six arms were used in this study (refer to **Table 1**). Two groups received Ad-IL-13, two groups received the control virus Ad-dl-70, and two received no virus. We included two groups receiving a control virus to determine whether the presence of an adenovirus alone is sufficient to alter barrier function. Three groups received the compound picrotoxin, which has previously been shown to prevent goblet cell metaplasia, while the other three groups received saline (Xiang et al., 2007). To keep the daily handling of all of the mice consistent we gave the mice not receiving picrotoxin a daily i.n. dose of saline at an equal volume that the picrotoxin mice receive their drug (50 µl). We expected that the picrotoxin will prevent any significant change in epithelial integrity compared to control (no virus groups) despite the presence of IL-13 due to the prevention of goblet cell metaplasia. Four mice were included in each group, for a total of 24 undergoing a lung clearance test.

Table I: Experimental arms

Group #	Virus type	Drug
1	Ad-IL-13	Saline control
2	Ad-dl-70	Saline control
3	No virus	Saline control
4	Ad-IL-13	Picrotoxin
5	Ad-dl-70	Picrotoxin
6	No Virus	Picrotoxin

In addition to assessing epithelial integrity, we measured several secondary outcomes. Airway hyperresponsiveness (AHR) to nebulized

methacholine was measured, as IL-13 overexpression has resulted in airway hyperresponsiveness in previous studies. We expected both groups receiving Ad-IL-13 to be hyperresponsive to methacholine. We removed the lungs and stained the tissue using the Periodic Acid-Schiff (PAS) protocol to quantify the number of goblet cells present in the airway, expecting just the Ad-IL-13 and saline group to have significantly increased levels of goblet cells. Using the supernatant from the bronchoalveolar lavage (BAL) fluid we performed an enzyme-linked immunosorbent assay (ELISA) to measure levels of IL-13. We included 9 mice per group undergoing all of the above mentioned secondary outcomes, for a total of 54 mice. Including the 24 mice involved in the lung clearance test, this study involved 78 mice.

CHAPTER 3: METHODOLOGY

3.1 Mice

All mice used in this study were female BALB/c mice, 8 – 10 weeks old and purchased from Charles River Laboratories (Saint-Constant, Quebec, Canada). They were housed in an environmentally controlled level II biohazard room throughout the experiment until outcome days. The experiment and all procedures were approved by the Animal Ethics Research Board at McMaster University, Hamilton, Ontario, Canada.

3.2 Adenovirus Preparation and Delivery

Each mouse was anesthetized with isoflurane and hung on an intubation board (Hallowell Engineering and Manufacturing, Pittsfield, MA). Masking tape was placed over the mouse's upper chest to position the airways correctly. An otoscope (Welch Allyn) with a 2.5" speculum attachment (Hallowell Engineering) was used as a visual aide to insert a blunt ended 22 gauge 1 inch Insyte IV catheter (BD) into the trachea. The blunted ended needle was removed from the catheter and 50ul of $1x10^8$pfu virus was administered into the mouse lungs through this inserted catheter. When all the fluid was administered the catheter was removed and the mouse taken off the intubation board and allowed to recover.

3.3 Picrotoxin and Saline Control Preparation and Delivery

Picrotoxin dose and concentration was administered as described by Xiang et al. (2007). Each mouse receiving picrotoxin was given an intranasal (i.n.) daily dose of 4.0μg of picrotoxin in 50μl of PBS for 10 days starting on the morning of adenovirus administration. Saline controls received 50μl of PBS and followed the same schedule as the picrotoxin administration.

3.4 Lung Clearance Test to Assess Epithelial Permeability

Our lung clearance test was performed using single photon emission computed tomography (SPECT) to track the movement of technetium-99m labeled diethylene triamine penta-acetate (^{99m}Tc-DTPA) out of the lungs. The DTPA, with a molecular mass of approximately 492Da, was instilled intratracheally and its clearance was assessed by imaging the mouse with a scintillation detector (that measures radiation) to observe the movement of the molecule throughout the body.

Before the lung clearance test the mice were sedated with an intraperitoneal (i.p.) injection of xylazine (10mg/kg at a concentration of 20mg/ml diluted in 1 x phosphate-buffered saline (PBS), Bayer HealthCare). Approximately five to ten minutes later a second i.p. injection of sodium pentobarbital (30mg/kg at a concentration of 54.7mg/ml diluted in 1 x PBS, Ceva Santé Animale, La Basille, PQ) was administered. Once sedated with no observable toe-pinch reflex, we performed a tracheotomy using a blunted 18-

guage needle as an endotracheal (ET) tube. The mice were ventilated at 150 breaths per minute using a rodent ventilator, and health status was monitored throughout by pulse oximetry. We then instilled approximately 250µCi ^{99m}Tc-DTPA through the catheter with a microsprayer before placing the mice in a GammaMedica-Ideas X-SPECT system (NorthRidge, California), that detects the radiation from the decaying Tc99m. Dynamic 2D planar images of the entire body were acquired over a 20 minute period at a rate of 1 frame every 30 seconds, for a total of 40 frames per mouse, displaying the intensity of the radiation. After 20 minutes the mice were removed from the SPECT machine and sacrificed by cervical dislocation.

The 40 frames per mouse of ^{99m}Tc-DTPA images were analyzed using Amide medical image analysis software (Free software foundation). We positioned a region of interest around the whole lung area, and the software then calculated the mean count per voxel within the region of interest for each frame. Among the 40 frames, the one with the highest count was set to 100% and all other frame counts were calculated as a percentage relative to this voxel. Data was plotted against time to produce a clearance rate graph. The area above the curve was determined for each mouse for comparison between groups.

3.5 Airway Responsiveness Measurements

The airway responsiveness to methacholine was performed using a *flexiVent* v5.2 rodent ventilator (SCIREQ, Montreal, Canada). Prior to airway

physiology measurements, the mice were anaesthetized with an i.p. injection of 10mg/kg of xylazine (Bayer HealthCare) at a concentration of 20mg/ml diluted in 1 x PBS. 5-10 minutes after the xylazine injection, a second i.p. injection of 30mg/kg of sodium pentobarbital (Ceva Santé Animale, La Basille, PQ) was given at a concentration of 54.7mg/ml diluted in 1 x PBS. Consistent with our methodology during the lung clearance test, we performed a tracheotomy using a blunted 18-guage needle as an ET tube once the mice were sedated with no observable toe-pinch reflex. Mice were connected to the *flexiVent* via the ET tube and ventilated at a rate of 150 breaths per minute. To prevent the mice from breathing against the ventilator, which would interfere with airway resistance measurements, 20mg/kg of the paralytic pancuronium bromide (Sandoz) was administered intraperitoneally at a concentration of 2mg/ml.

Methacholine (Sigma) was prepared by performing serial dilutions from a stock concentration in 1 x PBS. We administered concentrations of 0 (pure saline), 3, 6, 12, 25, and 50mg of methacholine/ml. Baseline respiratory resistance (R_{RS}), calculated by a pressure transducer that measures dynamic resistance, was performed before the first dose and every 30 seconds after each dose, for a total of 3 minutes per dose. Each dose of methacholine was administered for 10 seconds through a micropump nebulizer (Aerogen) during an inspiratory cycle. Heart rate and oxygen saturation were measured for the entire duration that the mouse was attached to the ventilator using an ear probe (Biox 3700, Ohmeda, Boulder, CO) measuring infrared pulse oxymetry that was placed

on the mouse's hind limb. After three minutes of data collection at the final dose the mouse was removed from the ventilator for further tissue collection.

The $\log_{10}$ of the nebulized concentration of methacholine was plotted vs. the peak resistance value at each concentration. Statistical significance was assessed by performing a t-test; P values less than 0.05 were considered significant.

3.6 Bronchoalveolar Lavage (BAL)

After airway physiology measurements, we opened the thorax exposing the lungs and heart. The mice were sacrificed by cutting the aorta resulting in exsanguination. We performed the BAL by injecting 250µl of PBS into the lungs via the ET tube that passed through the trachea. After five seconds the fluid was withdrawn from the lungs. This was repeated a second time with an additional 250 µl of BPS for a total volume of 500µl. The BAL fluid was centrifuged for 10 minutes at 1500 revolutions per minute (rpm) and the supernatant was removed and stored at -20°C. An ELISA was performed using the supernatant to determine the level of IL-13 in the BAL fluid.

The cell pellet was resuspended in 150µl of PBS to perform a total cell count. 20µl of Trypan Blue was added to 20µl of the suspension, and the resulting solution was placed on a hemocytometer for cell counting under a microscope. Live and dead cells were counted in all four quadrants of the hemocytometer and the total cell count was calculated.

An additional 150µl of PBS was added to the suspension in order to perform a cytospin (Cytospin 3; Shandon Scientific, Sewickly, PA). Three cytocentrifuge slides per sample were prepared and pre-wet with 85µl of PBS before adding 95µl of suspension per slide. After the cytospin the slides were allowed to dry overnight. To perform differential white blood cell counts the slides were stained with a Wright-Giemsa (Sigma) stain protocol. The slides were dehydrated with methanol and allowed to dry before the cell pelette area was covered with about two drops of Wright-Giemsa stain (W-G). After two minutes an equal amount of distilled water was added and mixed with the W-G thoroughly. After 3½ minutes the slides were rinsed with distilled water and left to air dry. The stained slides were coverslipped using Permount (Fisher Scientific) and left overnight to dry. Cell differential counts were performed by counting 400 cells under 40x magnification and classified as one of four types of white blood cells; macrophages, lymphocytes, neutrophils, and eosinophils.

3.7 Lung Histology to Quantify Goblet Cells in the Airways

Following airway resistance measurements and BAL collection, the lungs were dissected from the chest cavity of the mouse. The left and right lobes were separated and the right lung was frozen at -80°C. The left lung was inflated with 10% formalin at a pressure of 25cmH_2O, closed off at the trachea, and fixed in formalin for 24 hours. After fixation, the left lung was bisected and the inferior section was embedded in paraffin to obtain a transverse cross section of the

large airways. Three-micron thick sections were cut using a microtome and fixed to microscope slides. The slides were baked for 40 minutes at 70°C prior to staining with the Periodic Acid-Schiff (PAS) protocol that stains glycogen such as the mucin found in goblet cells purple and allowed us to quantify them in the airway.

The tissue was hydrated prior to staining by first removing sections of wax in xylene before being transferred into 100%, 95%, and eventually 70% ethanol solution, and finally in water. After being rinsed in distilled water, the tissue slides were placed in periodic acid (Sigma) for 12 minutes, washed and rinsed in distilled water, then placed in Schiff's reagent (Sigma) for 16 minutes. Tissue slides were washed and rinsed again in distilled water before being counterstained in Hematoxylin, rinsed and washed, placed in Tris Buffer pH 7.6 for one minute, rinsed and washed again, and dehydrated in increasing concentrations of ethanol. Finally, the slides were cleared in xylene and cover-slipped with Permount.

We collected images of the stained airway sections under magnification and digitally traced a line using a computer analysis system (Northern Eclipse, Version 7.0; Empix Imaging Inc., Mississauga, Ontario, Canada) along the basal surface of the epithelium to determine the length of the basement membrane of each sample. The number of positively stained goblet cells was individually

counted and expressed as the number of goblet cells per length of basement membrane (goblet cells/mm).

3.8 ELISA to Quantify IL-13 levels in the BAL Fluid

IL-13 levels in the BAL fluid were measured using a mouse IL-13 enzyme linked immunosorbent Assay (ELISA) kit (R&D Systems Inc., Minneapolis, MN). 20 wells of a 96-well microplate were coated with 100µl of the diluted capture antibody and left it at room temperature for 24 hours. The wells were washed and 300µl of reagent diluents were added to each well and left to incubate for 1 hour at room temperature.

The wells were washed again before adding 100µl of sample or standard in diluents in each well; using 4 samples from the Ad-IL-13 + saline group, 4 from the Ad-dl-70 + saline group, and 4 from the no virus + saline group. After 2 hours of incubation at room temperature the wells were washed and 100µl of detection antibody diluted in reagent diluents was added (1% bovine serum albumin in PBS) and left it to incubate for another 2 hours at room temperature. The wells were washed again and 100µl of Streptavidin-horseradish-peroxidase (HRP) was added to each well and allowed to incubate in a dark area for 20 minutes. The wells were washed before adding 100µl of substrate solution to each well, allowed to incubate for 20 minutes, then 50µl of stop solution was added and the microplate was gently tapped to mix the solution. Using a microplate reader set at 450nm with a 540nm correction, the software detected the optical density of

each well. Using the standard curve as a relative scale, the software calculated the level of IL-13 cytokine in pg/ml.

CHAPTER 4: RESULTS

4.1 Lung Clearance Test for Saline Groups

To determine any potential differences in the epithelial permeability, we performed a lung clearance test with the radio-labeled aerosol technetium-99m diethylene triamine penta-acetate (^{99m}Tc-DTPA) and measured its dispersion out of the lungs using single photon emission computed tomography (SPECT) over 20 minutes. Our first three groups of mice received Ad-IL-13 with daily doses of saline, Ad-dl-70 with daily doses of saline, or no virus with daily doses of saline, totaling 12 mice (4 per group). 2D images were taken every 20 minutes, for a total of 40 images total per mouse. See **Figure 2** for a representative image of a mouse from the Ad-IL-13 + saline group in 5 minute intervals (**Figure 2A**) compared to a mouse from the no virus + saline group (**Figure 2B**). The bright spots indicate areas of high radioactivity. After 20 minutes there appears to be very little difference between the two groups, and most of the radioactivity remains in the lungs. We quantified the dispersion by identifying a region of interest around the lung area and calculated the mean radioactivity count per voxel for each frame. **Figure 3** displays the clearance rate of the ^{99m}Tc-DTPA out of the region of interest (the lung area) over 20 minutes. Each data point represents the mean radioactivity of each mouse in the same group at a specific frame. Many of the data points lie on top of each other and after 20 minutes there is no significant difference between groups; each group has about 70%

radioactivity remaining in the region of interest relative to the maximum. We calculated the area above the curve (see **Figure 4**) represented in a bar graph. There was no statistical difference ($p<0.05$) among the three arms.

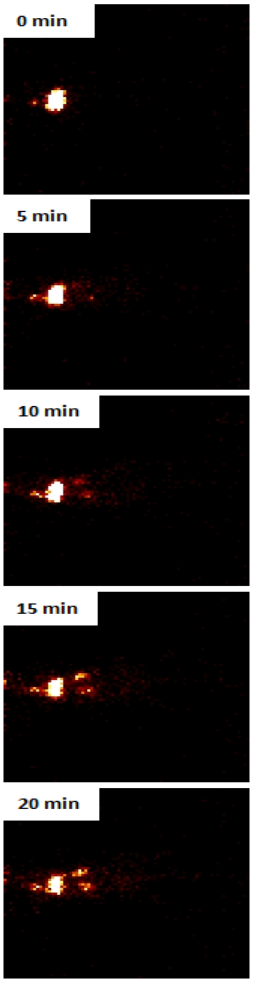

Figure 2A: ^{99m}Tc-DTPA dispersion in an Ad-IL-13 infected mouse

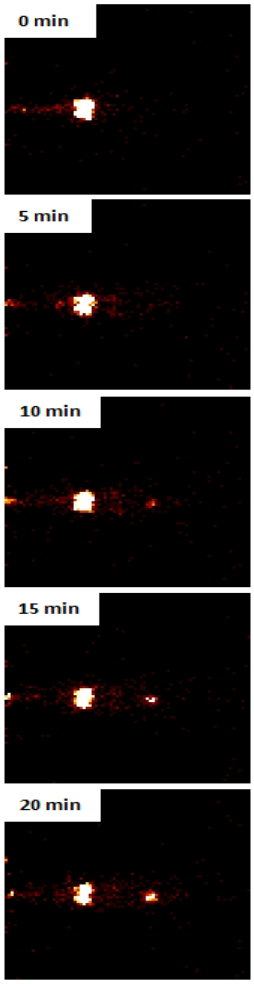

Figure 2B: ^{99m}Tc-DTPA dispersion in a control mouse with no virus

SPECT images of two sedated female BALB/c mice ventilated at 150 breaths per minute on a *flexiVent* rodent ventilator infected with Ad-IL-13 **(2A)** or not infected with a virus **(2B)**, and intratracheally instilled with ^{99m}Tc-DTPA. The bright areas indicate a high concentration of radioactivity. After 20 minutes of imaging, most of the radioactivity remains in the lung area. Sample size per group (n)=4 mice.

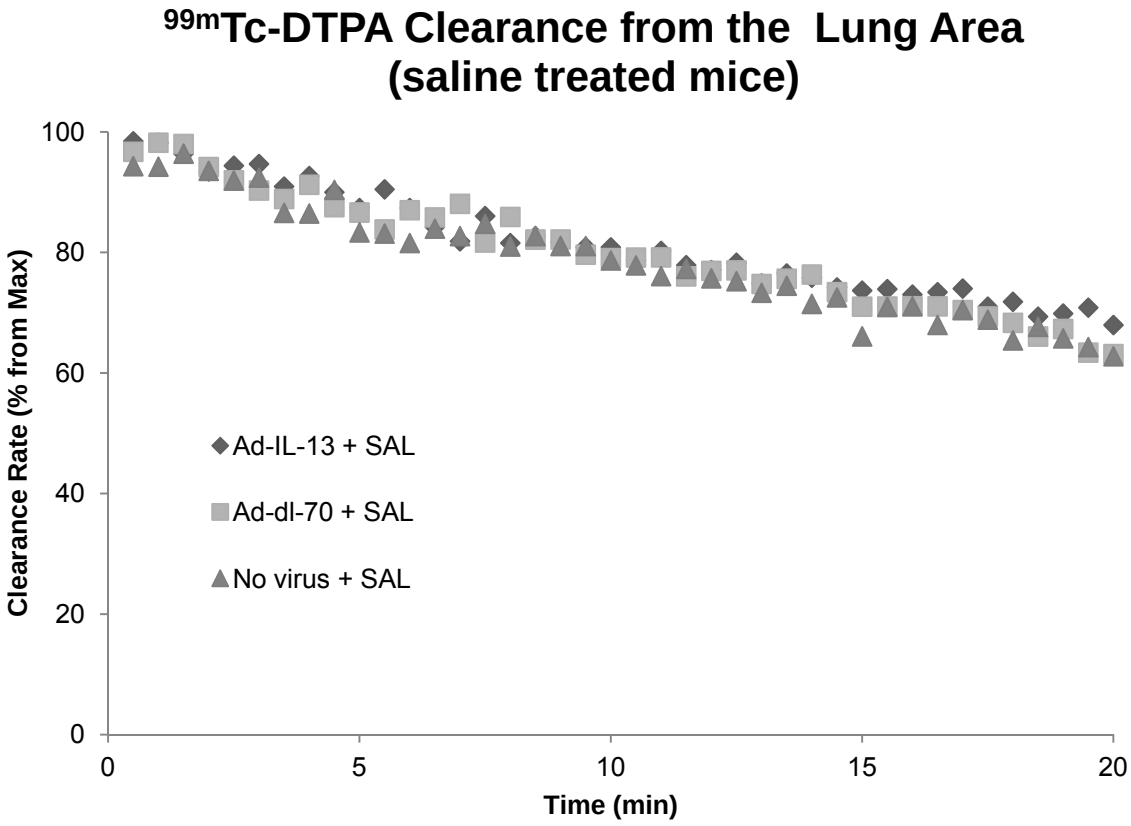

Figure 3: ^{99m}Tc-DTPA clearance over time in saline treated mice
Intratracheally instilled ^{99m}Tc-DTPA clearance out of the lung area over 20 minutes in Ad-IL-13 + daily saline (diamond data points), Ad-dl-70 + saline (square data points), and no virus + saline (triangle data points) female BALB/c mice 10 days after virus administration. Values are expressed as a percent of maximum baseline Tc99m radioactivity detected by the SPECT machine. Each data point represents the mean radioactivity of all the mice in a group at that specific time. The three curves decay at a similar rate and there is a large amount of overlap with no statistical significance among the final clearance values ($p>0.05$). Sample size per group (n)=4 mice.

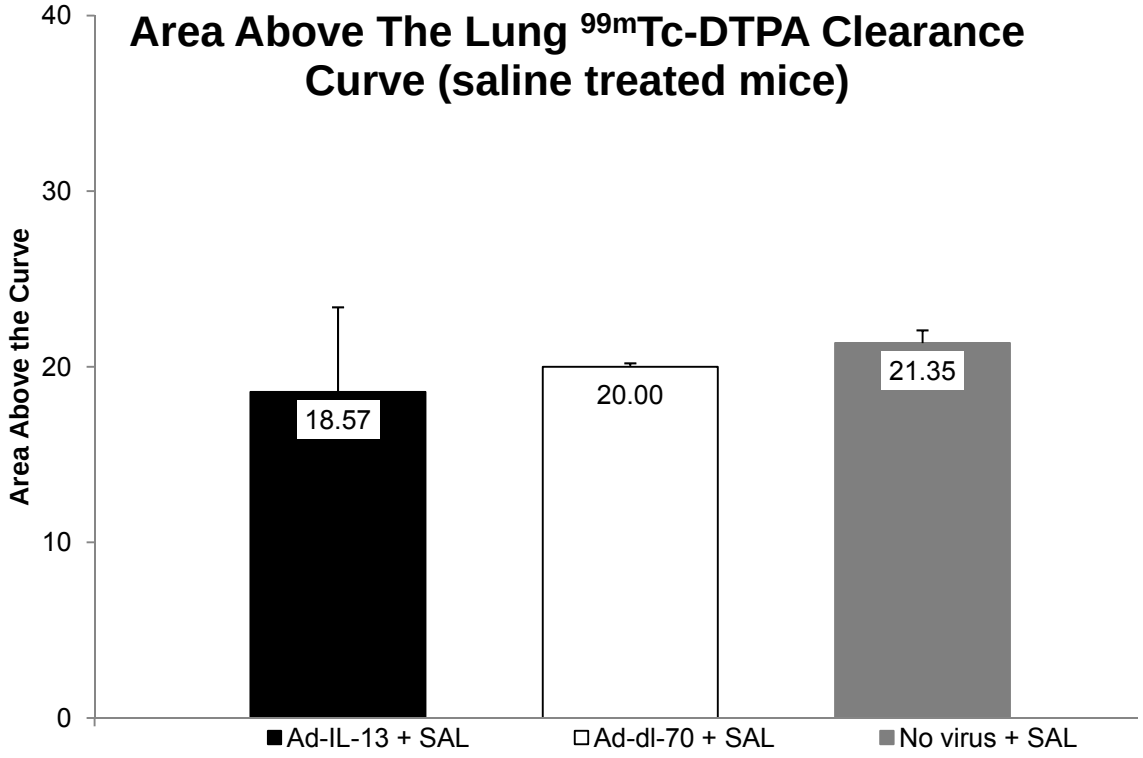

Figure 4: Area above the lung ^{99m}Tc-DTPA clearance curve over 20 minutes in saline treated mice

Comparison of the area above the curve of the ^{99m}Tc-DTPA clearance rate graph from baseline in Ad-IL-13 + saline (black), Ad-dl-70 + saline (white), and no virus + saline (grey) female BALB/c mice. After 20 minutes there was no significant difference among the three groups, indicated by a p value greater than 0.05. Error bars represent standard error of the mean. Sample size per group (n)=4 mice.

4.2 Lung Clearance Test for Picrotoxin Groups

We performed the same lung clearance test on an additional three arms; mice infected with Ad-IL-13 receiving daily doses of the $GABA_AR$ antagonist picrotoxin, Ad-dl-70 receiving daily doses of picrotoxin, or no virus receiving doses of picrotoxin, totaling 12 mice (4 per group). These groups allow us to compare lung clearance test results, under conditions that have shown in previous studies to prevent goblet cell metaplasia, to our previous three groups of mice that we imaged receiving daily doses of saline rather than picrotoxin (Xiang et al., 2007). Consistent with the previous groups of mice, we imaged the dispersion of ^{99m}Tc-DTPA out of the lung area using SPECT over 20 minutes. The 2D SPECT images looked identical to the ones of the three saline treated groups (see **Figure 2A** and **2B** for a sample comparison) with a large amount of radiation remaining in the lung area after 20 minutes. We quantified the dispersion by identifying a region of interest around the lung area and calculated the mean radioactivity count per voxel for each frame. **Figure 5** displays the clearance rate of the ^{99m}Tc-DTPA out of the region of interest (the lung area) over 20 minutes in the three picrotoxin treated arms. Each data point represents the mean radioactivity of all the mice in the same group at a specific frame (every 30 seconds after baseline measurements). Similar to the trend observed in the three saline treated arms, many of the data points lie on top of each other and after 20 minutes there is no significant difference between groups(p value was greater than 0.05); each group has about 65% radioactivity remaining in the

region of interest relative to the maximum. We calculated the area above the curve (see **Figure 6**) represented in a bar graph. There was no statistical difference ($p>0.05$) among the three arms. We compared these results to the area above the curve in the three saline treated groups and also did not find any statistical significance ($p>0.05$). See **Figure 7** for a comparison of the ^{99m}Tc-DTPA clearance out of the lungs in the two groups receiving Ad-IL-13 (Ad-IL-13 + saline and Ad-IL-13 + picrotoxin) and **Figure 8** for the area above the curve for these two groups, which were of particular interest because we expected a significant difference in the epithelial permeability between these two groups; however, the rate of ^{99m}Tc-DTPA clearance out of the region of interest was similar (around 70% clearance after 20 minutes).

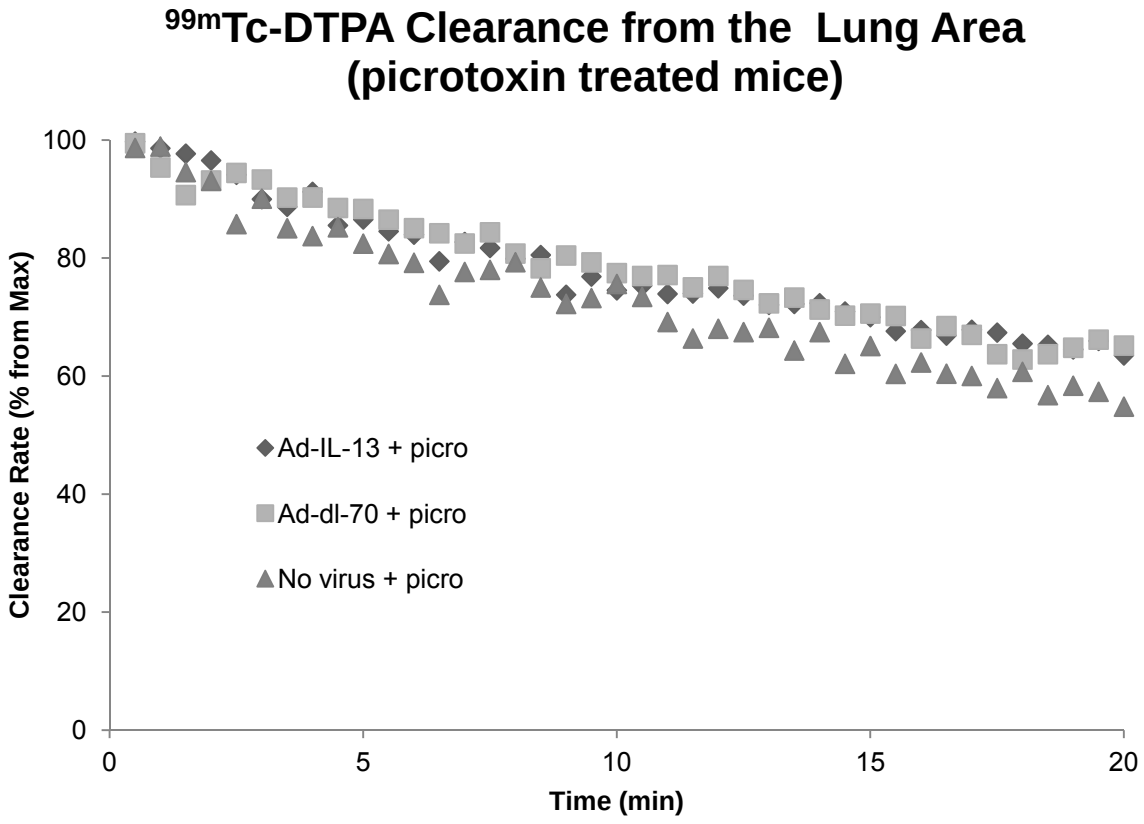

Figure 5: ^{99m}Tc-DTPA clearance over time in picrotoxin treated mice
Intratracheally instilled ^{99m}Tc-DTPA clearance out of the lung area over 20 minutes in Ad-IL-13 + daily picrotoxin (diamond data points), Ad-dl-70 + picrotoxin (square data points), and no virus + picrotoxin (triangle data points) female BALB/c mice. Values are expressed as a percent of maximum baseline Tc99m radioactivity detected by the SPECT machine. Each data point represents the mean radioactivity of all the mice in a group at that specific time. The three curves decay at a similar rate and there is a large amount of overlap with no statistical significance among the final clearance values ($p>0.05$). Sample size per group (n)=4 mice.

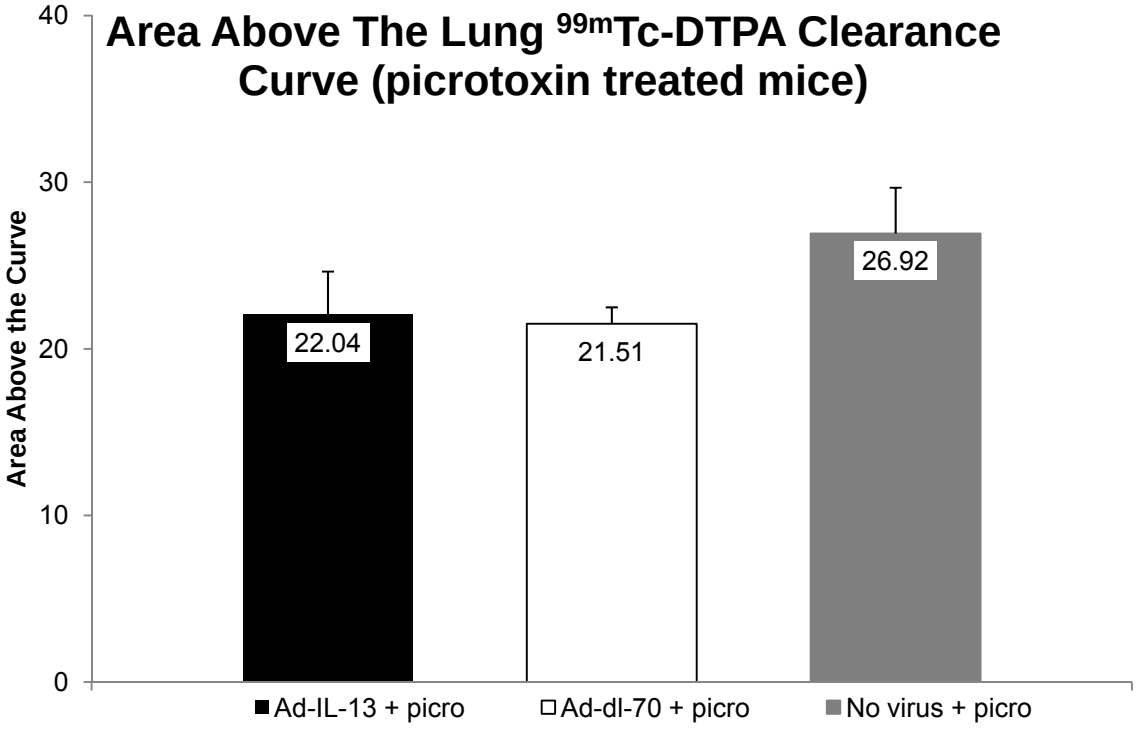

Figure 6: Area above the lung ^{99m}Tc-DTPA clearance curve over 20 minutes in picrotoxin treated mice

Comparison of the area above the curve of the ^{99m}Tc-DTPA clearance rate graph from baseline in Ad-IL-13 + picrotoxin (black), Ad-dl-70 + picrotoxin (white), and no virus + picrotoxin (grey) female BALB/c mice. After 20 minutes there was no significant difference among the three groups, indicated by a p value greater than 0.05. Error bars represent standard error of the mean. Sample size per group (n)=4 mice.

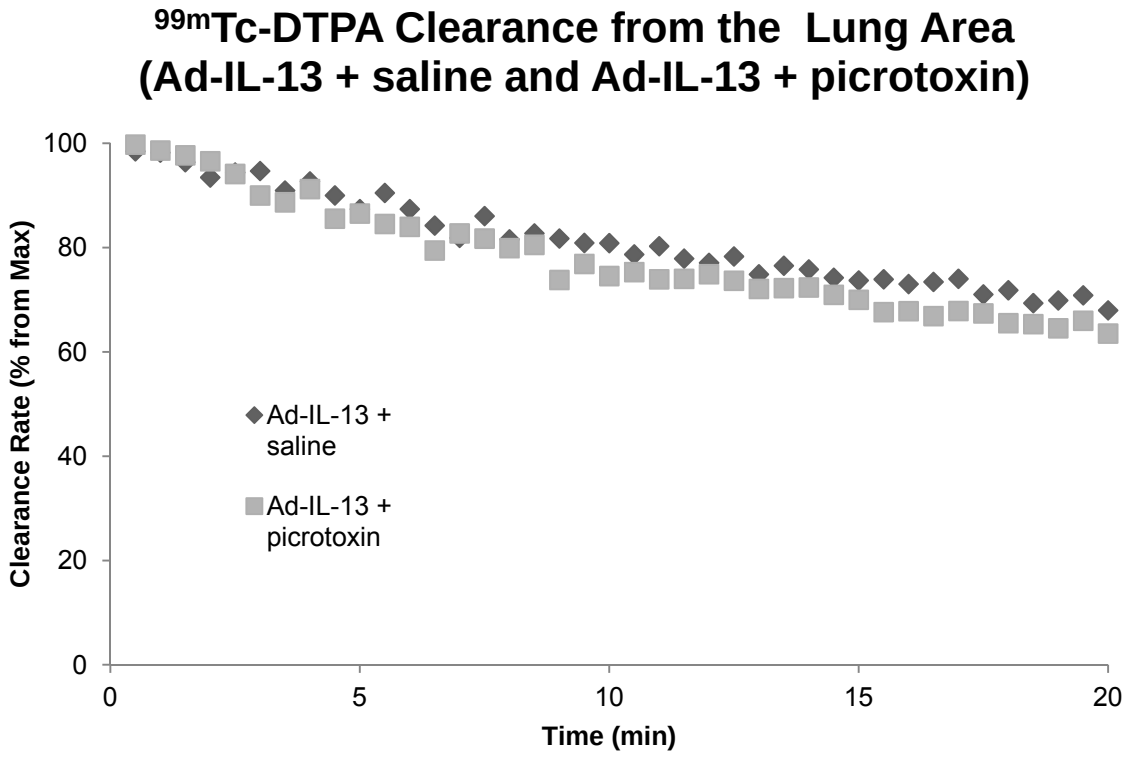

Figure 7: ^{99m}Tc-DTPA clearance over time in Ad-IL-13 + saline and Ad-IL-13 + picrotoxin treated mice

Intratracheally instilled ^{99m}Tc-DTPA clearance out of the lung area in Ad-IL-13 + saline (diamond data points) and Ad-IL-13 + picrotoxin (square data points) treated BALB/c mice. Values are expressed as a percent of maximum baseline Tc99m radioactivity detected by the SPECT machine. Each data point represents the mean radioactivity of all the mice in a group at that specific time. After 20 minutes, there was no significant difference in ^{99m}Tc-DTPA clearance between these two groups ($p>0.05$); there is about 70% radioactivity remaining in the lung area. Sample size per group (n)=4 mice.

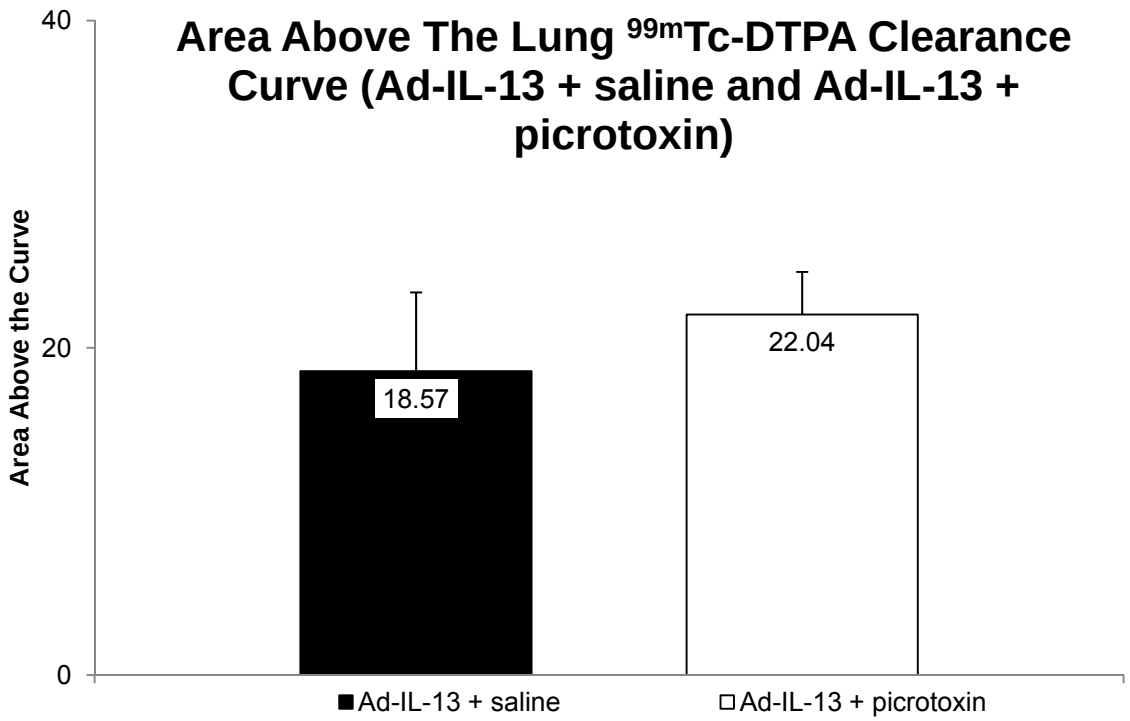

Figure 8: Area above the lung ^{99m}Tc-DTPA clearance curve over 20 minutes in Ad-IL-13 + saline and Ad-IL-13 + picrotoxin mice

Comparison of the area above the curve of the ^{99m}Tc-DTPA clearance rate graph between Ad-IL-13 + saline (blue) and Ad-IL-13 + picrotoxin (red) treated female BALB/c mice from baseline. After 20 minutes there was no significant difference between these two groups ($p>0.05$). Error bars represent standard error of the mean. Sample size per group (n)=4 mice.

4.3 Goblet Cells

To quantify the number of goblet cells in the airway we fixed lung sections (three microns thick) from each mouse to microscope slides and stained them with the Periodic Acid-Schiff (PAS) protocol (see **Figure 9** for a representative image of a lung tissue section from each group stained by PAS technique). This technique stains the mucin-containing goblet cells purple. We expressed the number of positively stained goblet cells (counted individually) per length of basement membrane (in millimeters). The Ad-IL-13 + saline group had a mean goblet cell count of 42.62 goblet cells/mm, significantly greater than the Ad-dl-70 (1.67 goblet cells/mm; only one mouse had a positive PAS stain) and the no virus + saline mice (0 positively stained airway goblet cells among all the mice in this group). The Ad-IL-13 + picrotoxin mice also had a significantly greater number of goblet cells (40.7) compared to the other picrotoxin-treated mice (0 positively stained airway goblet cells in both the Ad-dl-70 + picrotoxin and no virus + picrotoxin groups). There was no significant difference between the Ad-IL-13 + saline and Ad-IL-13 + picrotoxin groups (42.62 and 40.7 goblet cells/mm, respectively. Statistical significance was determined by a t test with a p value of less than 0.05. See **Figure 10** for the quantification of the mean goblet cell numbers per group.

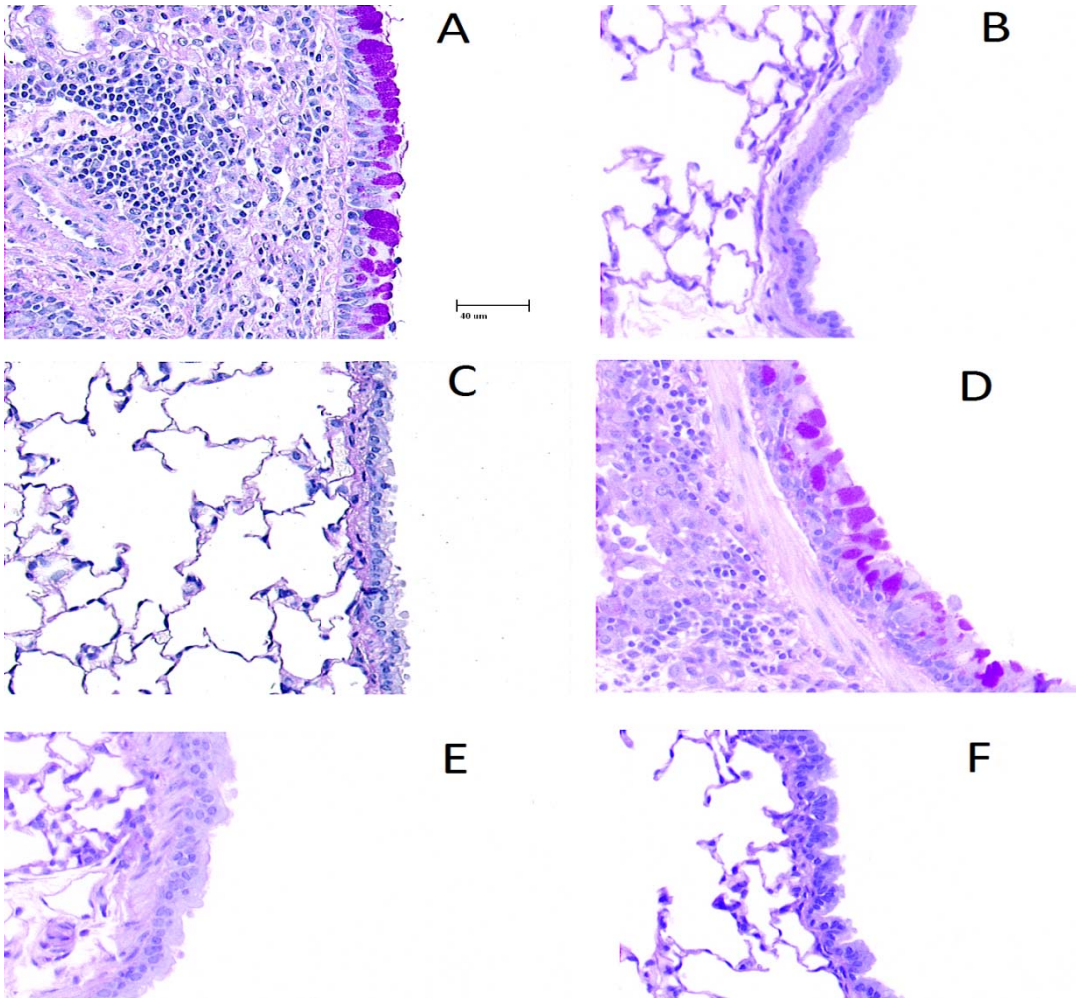

Figure 9: PAS stain of lung tissue section

A representative image of a PAS stained lung tissue section from each group of female BALB/c mice 10 days after infection at 40x magnification: Ad-IL-13 + daily saline (A) Ad-dl-70 + saline (B), no virus + saline (C), Ad-IL-13 + daily picrotoxin (D), Ad-dl-70 + picrotoxin (E), and no virus + picrotoxin (F). The purple cells along the airway epithelium (facing the airway lumen to the right of the lung tissue) in figure A and D are goblet cells positively stained by the PAS technique. Beneath the basement membrane, in the parenchyma of the tissue in figure A and D is a buildup of inflammatory cells. Figures B, C, E, and F do not have a positive stain for goblet cells, and have virtually no buildup of inflammatory cells.

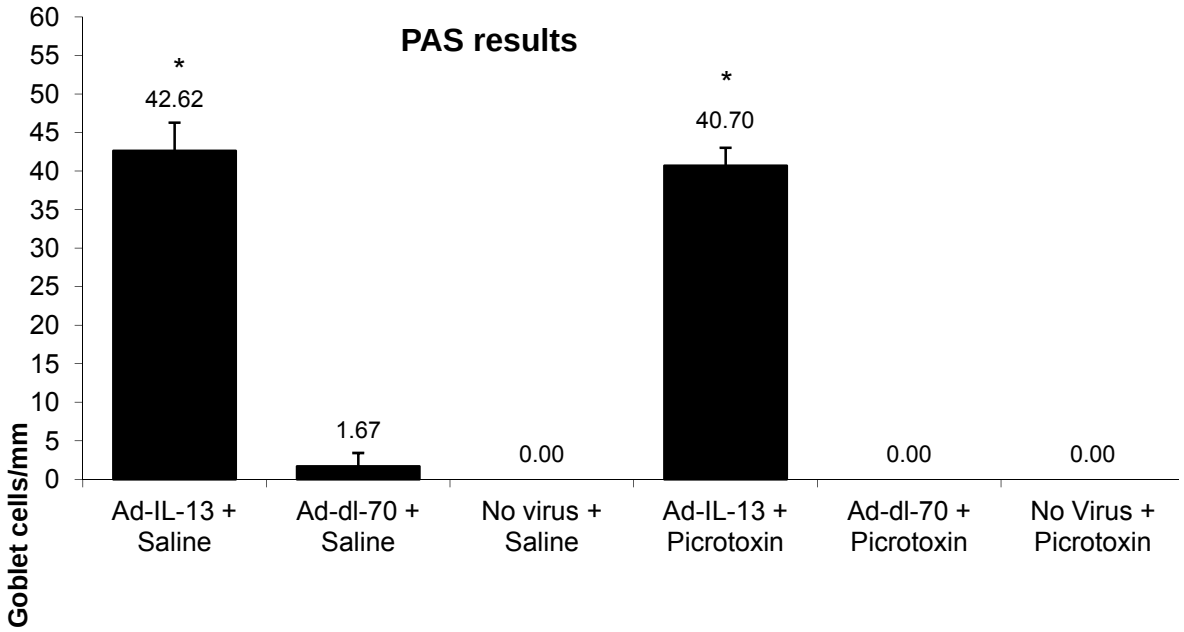

Figure 10: Quantification of goblet cells

Quantification of the mean number of goblet cells per group. Both groups infected with Ad-IL-13 (receiving either daily doses of saline or picrotoxin) had a significantly higher (indicated by the asterisks) number of goblet cells compared to the other 4 groups. There was no significance between the Ad-IL-13 + saline (mean of 42.62 goblet cells/mm) and the Ad-IL-13 + picrotoxin (mean of 40.7 goblet cells/mm) groups. Statistical significance was determined by a t test with a p value less than 0.05. Error bars represent standard error of the mean. Sample size per group (n)=9 mice.

4.4 Cell Differentials in the Bronchoalveolar Lavage (BAL)

After staining the BAL fluid cell pellet with W-G, 400 cells per mouse were counted under a microscope and identified as one of four types of white blood cells; macrophages, lymphocytes, neutrophils, and eosinophils (see **Figure 11**). Total cells, lymphocytes, neutrophils, and eosinophils were proportionally increased in the two groups of mice receiving Ad-IL-13.

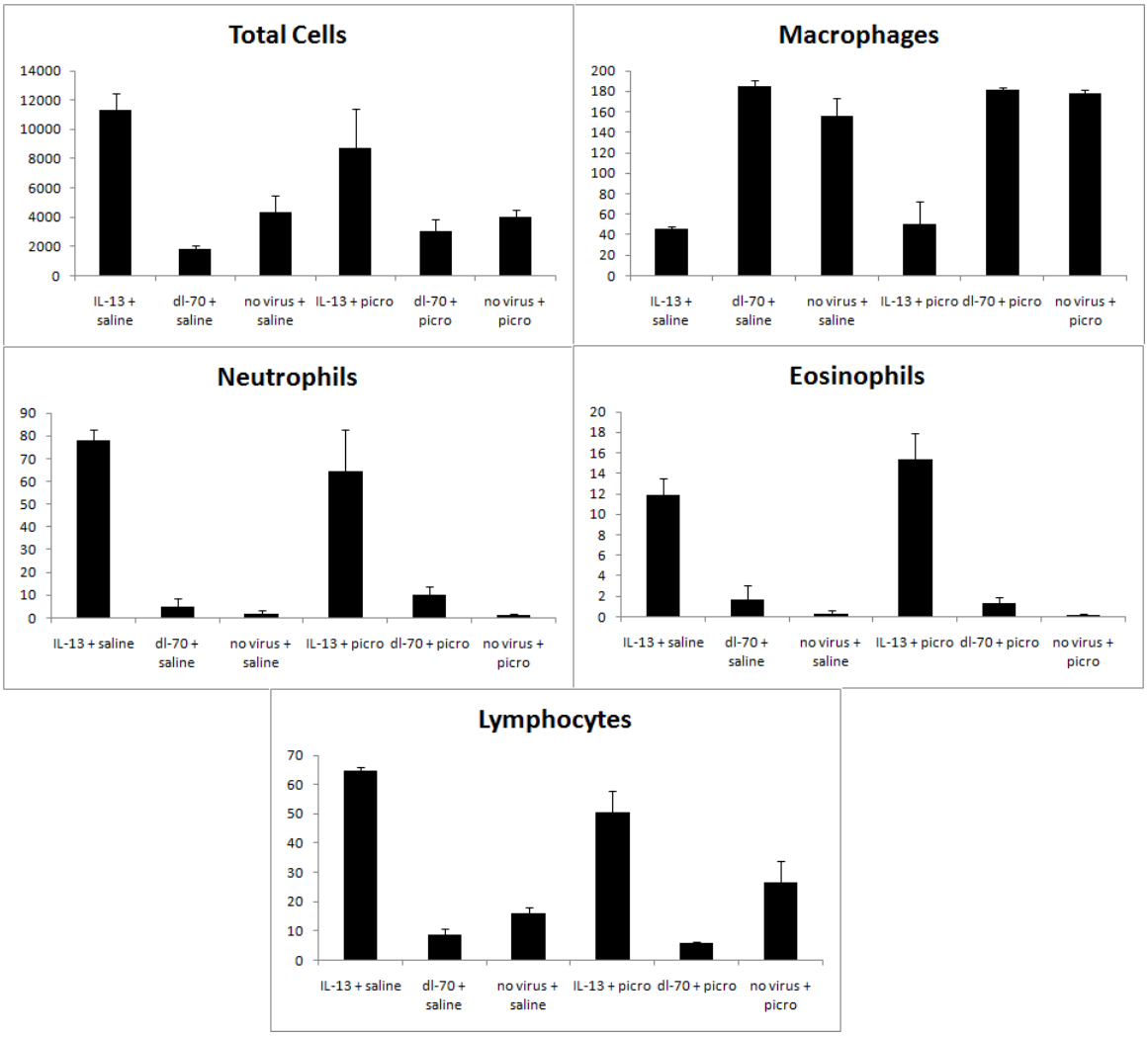

Figure 11: Total and Differential Inflammatory Cells in Bronchoalveolar Lavage Fluid

Total and differential inflammatory cell counts in the BAL fluid for all groups. Values are represented as a mean with error bars representing standard error of the mean. Sample size per group (n)=9 mice.

4.5 Airway Responsiveness Measurements

To assess the airway resistance to increasing doses of an airway smooth muscle agonist, increasing doses of methacholine was nebulized on a *flexiVent* rodent ventilator and total airway resistance was measured. The two groups infected with Ad-IL-13 (with daily doses of saline and daily doses of picrotoxin) averaged significantly increased total airway resistance ($p<0.05$) compared to the four other groups. See **Figure 12** for a dose response curve from the three groups receiving daily saline, **Figure 13** for the three groups receiving daily picrotoxin, and **Figure 14** for the four groups receiving adenovirus (either Ad-IL-13 or Ad-dl-70). A comparison of the Ad-IL-13 + saline and Ad-IL-13 + picrotoxin groups did not show statistical significance.

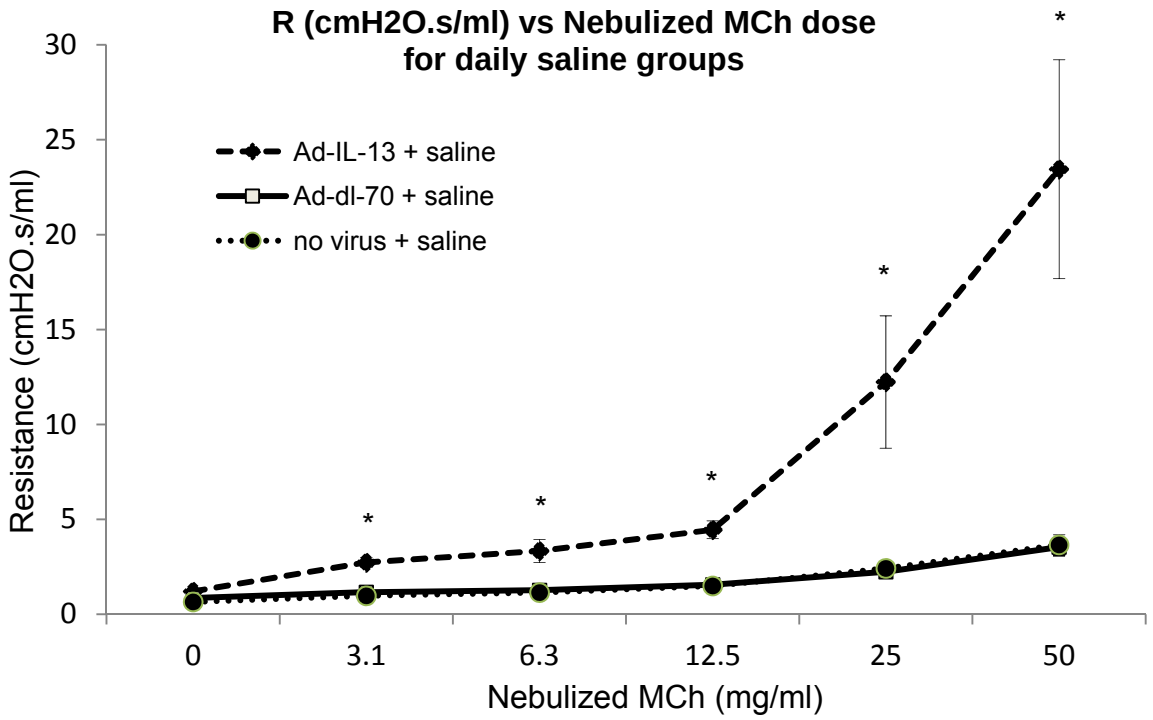

Figure 12: Resistance vs. nebulized methacholine dose response curve for saline treated mice

Measurement of airway responsiveness to nebulized methacholine in female BALB/c mice infected with Ad-IL-13, Ad-dl-70, or no virus all receiving daily doses of saline. There was no statistical significance among the Ad-dl-70 and the no virus group of mice; the curves overlap at all doses of methacholine. There was a statistically significant increase (indicated by the asterisks) in the resistance values for the Ad-IL-13 mice at 3.1mg/ml of methacholine and higher, up to 50 mg/ml inclusive. Error bars represent standard error of the mean, significance was attributed at a p value greater than 0.05. Sample size per group (n)=9 mice.

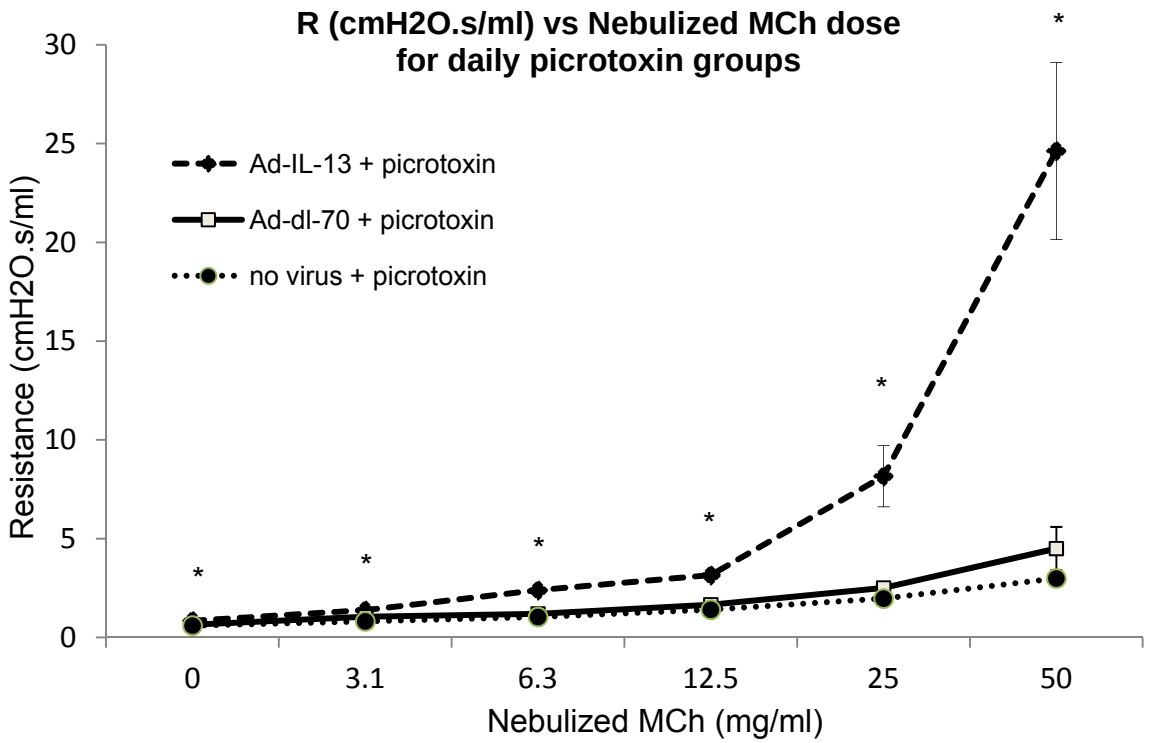

Figure 13: Resistance vs. nebulized methacholine dose response curve for picrotoxin treated mice

Measurement of airway responsiveness to nebulized methacholine in female BALB/c mice infected with Ad-IL-13, Ad-dl-70, or no virus all receiving daily doses of picrotoxin. There was no statistical significance among the Ad-dl-70 and the no virus group of mice; the overlap of the curves is not as tight as the Ad-dl-70 and no virus groups receiving saline as shown in **Figure 11**, however there is no statistical significance. There was a statistically significant increase (indicated by the asterisks) in the resistance values for the Ad-IL-13 mice at baseline and throughout all doses of methacholine. Error bars represent standard error of the mean, significance was attributed at a p value greater than 0.05. Sample size per group (n)=9 mice.

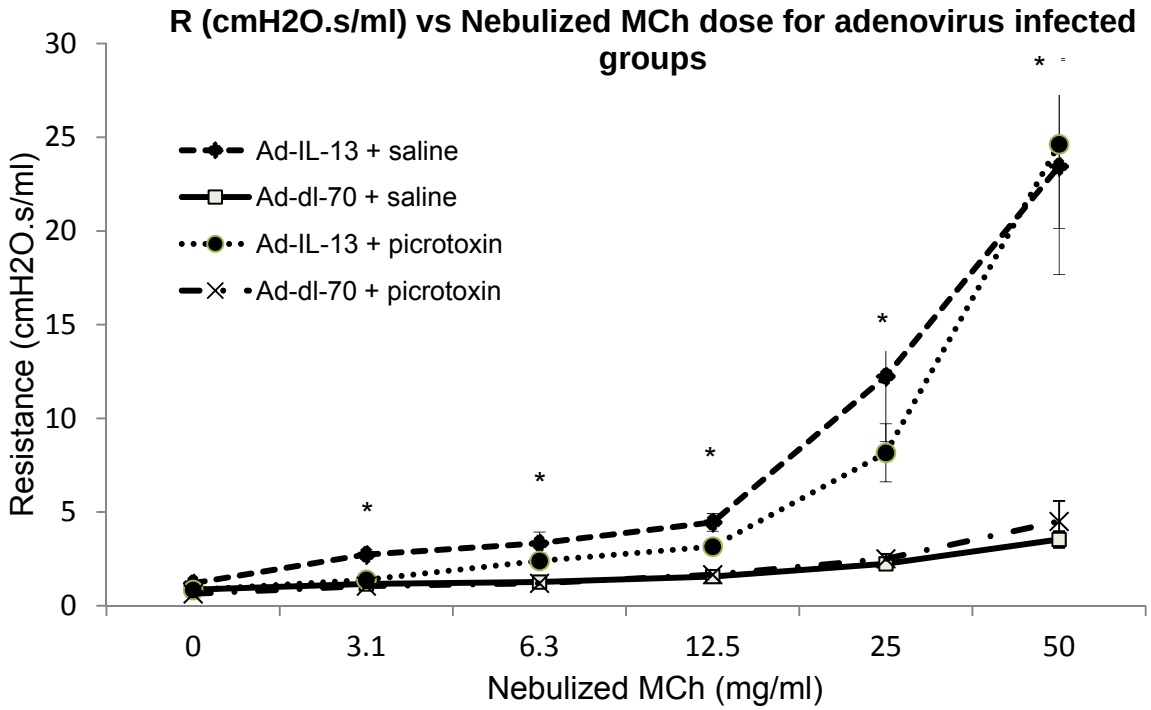

Figure 14: Resistance vs. nebulized methacholine dose response curve for adenovirus infected mice

Measurement of airway responsiveness to nebulized methacholine in female BALB/c mice infected with Ad-IL-13 + saline and + picrotoxin, and Ad-dl-70 + saline and + picrotoxin. There was no statistical significance among the two Ad-IL-13 groups and among the two Ad-dl-70 groups. There was a statistically significant increase (indicated by the asterisks) in the resistance values for the two Ad-IL-13 groups at 3.1mg/ml and throughout all doses of methacholine up to 50mg/ml inclusive compared to the two Ad-dl-70 groups. Error bars represent standard error of the mean, significance was attributed at a p value greater than 0.05. Sample size per group (n)=9 mice.

4.6 IL-13 ELISA Results

The IL-13 levels in the bronchoalveolar lavage (BAL) fluid were measured by ELSA from the Ad-IL-13 + saline, Ad-dl-70 + saline, and no virus + saline groups; from 4 mice per group. The average concentration per group is displayed in **Figure 15**. The average Ad-IL-13 + saline levels of IL-13 were significantly higher ($p<0.05$) than the average concentration from the Ad-dl-70 and no virus groups with an average concentration of 2656pg/ml compared to 275pg/ml and 265pg/ml, respectively.

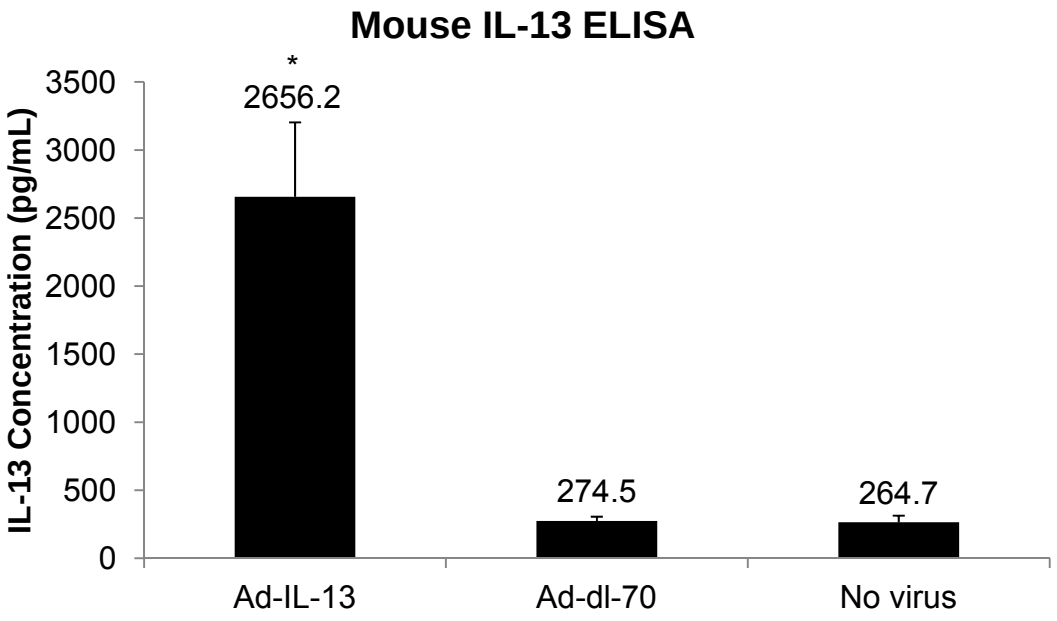

Figure 15: IL-13 levels from the BAL fluid from saline treated groups
Average IL-13 levels in the BAL in female BALB/c mice from the Ad-IL-13 + saline, Ad-dl-70 + saline, and no virus + saline groups. Concentration of IL-13 from the Ad-IL-13 group was significantly higher (indicated by the asterisk) than the two other groups ($p<0.05$). Sample size per group (n)=4 mice.

CHAPTER 5: DISCUSSION

5.1 Summary of Purpose and Results

The aim of this study was to determine whether goblet cell metaplasia, the transformation of epithelial cells into goblet cells, compromises epithelial barrier function and increases the permeability to aerosols such as diethylene triamine penta-acetate (DTPA). We hypothesized that goblet cell metaplasia would result in impaired barrier function and increased permeability to DTPA.

To test this hypothesis we developed an animal model using female BALB/c mice. We induced goblet cell metaplasia by administering an adenovirus to overexpress the cytokine IL-13. As a control we had a group of naïve mice that did not receive a virus and a group of mice receiving a control virus, to account for any changes induced by an adenovirus infection. Both the Ad-IL-13 and Ad-dl-70 viruses are replication deficient. Effects of the Ad-IL-13 in mouse airways have been shown to peak at 7 days and remain elevated for three days before declining towards baseline levels. Therefore, we chose to measure outcomes 10 days post virus infection.

To be able to attribute any observed changes in barrier function to goblet cell metaplasia, and not to any of the other factors affected by IL-13 overexpression, we included three more groups; Ad-IL-13 receiving daily doses of picrotoxin, Ad-dl-70 + daily doses of picrotoxin, and no virus + daily doses of picrotoxin, the latter two groups as a control to determine if adding the drug

picrotoxin affects our outcomes. To keep the handling of all groups of mice consistent, we gave daily doses of saline to the first three groups of mice so that all groups received daily i.n. treatment. The Ad-IL-13 group of mice receiving picrotoxin should have all of the physiological changes induced by IL-13 except for goblet cell metaplasia, which should be suppressed by the picrotoxin. This allows us to implicate the presence of goblet cells should this group of mice show different results to our tests compared to the Ad-IL-13 + saline group of mice.

We found that IL-13 overexpression induced many of the physiological changes expected including increased IL-13 levels in the BAL fluid, goblet cell metaplasia, and airway hyperresponsiveness to methacholine. However, we did not observe any changes to the permeability to ^{99m}Tc-DTPA in IL-13 overexpressed mice compared to control. Surprisingly, we did not observe any suppression of goblet cells in our Ad-IL-13 + daily picrotoxin group of mice.

5.2 IL-13 Levels in the Bronchoalveolar Lavage (BAL) Fluid

We performed an ELISA on the BAL fluid to measure levels of mouse IL-13 in the supernatant. We performed this test to confirm that we did indeed achieve IL-13 overexpression. We performed the ELISA on three groups of mice; Ad-IL-13 + saline, Ad-dl-70 + saline, and no virus + saline, as all of the adenovirus mice were infected on the same day, from the same batch of virus, keeping everything consistent among all mice. Therefore, the groups receiving picrotoxin should be equivalent to their saline treated counterparts. As expected,

average IL-13 levels were significantly higher in the Ad-IL-13 mice compared to the Ad-dl-70 and no virus groups of mice. This confirms the administration of Ad-IL-13 did induce IL-13 overexpression in our mice and that IL-13 levels in the control groups were significantly lower. We decided to measure IL-13 levels to confirm the virus was functionally active in the mouse airways. Had there been no significant difference between the Ad-IL-13 group and the other two groups our remaining results would be in question. Since the ELISA demonstrated that IL-13 levels did increase, we need to demonstrate that they achieved goblet cell hyperplasia in our Ad-IL-13 + saline group of mice by examining the Periodic Acid-Schiff (PAS) stained lung tissue.

5.3 Increased Goblet Cell Count in the Airways of Ad-IL-13 Mice

With IL-13 levels increased we expected goblet cell numbers to be elevated in the airways of our Ad-IL-13 + saline mice. After removing and embedding the lung tissue we fixed them to microscope slides and stained them with the PAS protocol. After collecting images of the primary airway and manually counting the number of goblet cells, we demonstrated that the Ad-IL-13 + saline mice had significantly increased goblet cell expression, as expected. Our Ad-dl-70 + saline group only had one mouse where we counted any goblet cells, and our no virus + saline group had a complete absence of goblet cells among all of the mice. Therefore, the Ad-IL-13 successfully increased goblet cell numbers in our mice and our model can appropriately be used to address our hypothesis.

When we examined our three picrotoxin treated groups, we did not observe any goblet cells in the Ad-dl-70 + picrotoxin or the no virus + picrotoxin groups, as expected. However, the picrotoxin failed to suppress goblet cell transformation in the Ad-IL-13 + picrotoxin group; goblet cell numbers were nearly identical to those of the Ad-IL-13 + saline group. It is not clear why picrotoxin at the same dose, with the same route of administration, and in the same species of mouse as in the 2007 *Nature Medicine* paper did not suppress goblet cell numbers as reported by Xiang and colleagues (Xiang et al., 2007). Based on the reported function of picrotoxin as a GABA A receptor blocker in the airway epithelium, there should have been a significant decrease in the number of goblet cells in the Ad-IL-13 + picrotoxin group compared to the Ad-IL-13 + saline group.

The main difference between the model used by Xiang and colleagues and the model we used in this experiment is how IL-13 was administered to increase goblet cell numbers. Xiang et al. administered 0.5μg in 40μl of recombinant IL-13 by i.n. application on the first, third, and fifth day of their experiment, before outcome measurements were performed on the sixth day (Xiang et al., 2007). As with our protocol, they administered 0.2μg per gram of body weight in 50μl of daily picrotoxin starting on the first day of IL-13 treatment by i.n. application. Both of these methods of overexpressing IL-13 are well established in animal research and are preferred over transgenenic models when it is desired to have the animal develop and mature to adulthood in the absence

of inserted or altered genes. Both our study and the study by Xiang and colleagues successfully achieved increased goblet cell expression. We cannot directly compare goblet cell numbers as they did not report the number of goblet cells per length of basement membrane as we did; however, they reported the histological mucus index (HMI), which indicates the proportion of mucus-producing cells in the epithelium, was similar in the recombinant IL-13 group to OVA treated mice and significantly higher compared to IL-13 mice receiving daily doses of picrotoxin. Therefore, the intended result of increasing goblet cell expression was achieved in both studies by different means of IL-13 overexpression.

IL-13 overexpression by adenovirus transfer does appear to produce higher levels of the cytokine compared to delivering recombinant IL-13 as performed in the *Nature Medicine* paper (Xiang et al., 2007). The levels of IL-13 in the BAL fluid as reported by Xiang and colleagues are around 100pg/ml in all IL-13 groups, including those receiving picrotoxin. This is about 25 times less than the amount of IL-13 measured in our Ad-IL-13 group of mice. The adenovirus, as used in our study, produces IL-13 constantly for 10 days (hitting a peak at 7 days) while Xiang et al. administered three doses of IL-13, which likely accounts for the lower levels of IL-13 measured in the BAL fluid in our study compared to their study. It may be possible that the increased IL-13 levels in our model completely overwhelmed the ability of picrotoxin to suppress goblet cell numbers; however, this seems unlikely as the goblet cell count was nearly

identical in our two Ad-IL-13 groups and not at all attenuated in the Ad-IL-13 + picrotoxin group. By not suppressing goblet cell metaplasia in our Ad-IL-13 + picrotoxin group of mice, our ability to assess the effect of preventing goblet cell metaplasia on epithelial barrier dysfunction is compromised. However, our model can still be used to measure changes to the barrier function under conditions of goblet cell metaplasia.

5.4 Airway Hyperresponsiveness in Ad-IL-13 Mice

The increased IL-13 in our two Ad-IL-13 groups in our study resulted in significant changes in the airway responsiveness to nebulized methacholine. There is clear evidence of increased airway hyperreactivity, and even a slight shift of the responsiveness curve to the left indicating airway hypersensitivity. This test demonstrates that IL-13 overexpression in both the saline and picrotoxin treated groups resulted in airway hyperresponsiveness, and that the administration of the control adenovirus (Ad-dl-70) did not affect airway physiology. When taking into consideration the increased levels of IL-13 in the BAL fluid and the increased number of airway goblet cells, we have evidence that IL-13 overexpression resulted in the expected functional changes based on known IL-13 activity in the airways of our Ad-IL-13 mice that represent the contributions of elevated levels of this cytokine to human asthma (Venkayya et al., 2002).

The consequences of administering a control adenovirus appears to have little impact on the ELISA, histology, and physiology outcomes we obtained, as the values for the Ad-dl-70 group of mice are not significantly different from our no virus groups of mice. Additionally, the daily dose of picrotoxin did not significantly affect any of our recorded results. Therefore, we are attributing differences in our Ad-IL-13 groups to the overexpression and downstream changes in the airway environment of the cytokine IL-13.

5.5 IL-13 Overexpression Did Not Significantly Alter Airway Barrier Function

5.5.1 Summary of Lung Clearance Test

We performed a lung clearance test measuring the dispersion of ^{99m}Tc-DTPA to determine whether the airway barrier function was compromised. We were working under the hypothesis that the goblet cell metaplasia we observed due to IL-13 overexpression would result in a significantly increased rate of ^{99m}Tc-DTPA clearance out of the lung area over 20 minutes in our Ad-IL-13 + saline group of mice compared to our two control groups. Based on our SPECT imaging results, the Ad-IL-13 + saline mice had an average dispersion similar to our two other saline control groups (Ad-dl-70 + saline and no virus + saline). Therefore, IL-13 induced goblet cell metaplasia did not significantly alter the ^{99m}Tc-DTPA clearance out of the lung area after 20 minutes in our mouse model.

5.5.2 Differences Between In Vitro and In Vivo Models of Barrier Function

Decreased tight junction proteins have been associated with epithelial permeability (Claude and Goodenough, 1973) and adjacent goblet cells have been associated with fewer tight junction proteins compared to adjacent epithelial cells (Matsumura and Setoguti, 1989). This evidence, along with the Lachowicz-Scroggins study that demonstrated a decreased transepithelial resistance after goblet cell metaplasia in cultured human epithelial cells, formed the basis of our hypothesis (Lachowicz-Scroggins et al., 2010). However, our results lead us to believe that goblet cell metaplasia alone does not impair epithelial barrier function *in vivo*. The Matsumara and Steoguti and the Lachowicz-Scroggins studies that examined the consequences of increased goblet cell expression in the epithelium did so in an isolated *in vitro* experiment. When isolated, it is possible that goblet cell metaplasia alone can contribute to an impaired or leaky airway epithelium, but *in vivo* there are mechanisms that prevent damage or restore the epithelial barrier function when goblet cell numbers are increased. It is important to keep in mind that the *in vitro* airway environment is different and more complicated compared to examining tissue *in vitro*.

A discrepancy among the results from *in vitro* vs. *in vivo* models has occurred with experiments performed in our lab in the past, and serve as a reminder that trends observed in isolated tissue cannot always be generalized to whole body conditions. As part of her 2009 thesis project, Jodie Powdrill

examined the contribution of house dust mite (HDM), a common allergen known to exacerbate asthma in sensitized individuals, to the airway barrier dysfunction observed in asthma. She was working under the hypothesis that exposure to HDM will damage the epithelium and enhance epithelial permeability, using the same lung ^{99m}Tc-DTPA clearance test we used in this study (Turi et al., 2011). Her hypothesis was based on *in vitro* data reported in two papers by Wan and colleagues (Wan et al., 1999; Wan et al., 2001). The 1999 paper published in *The Journal of Clinical Investigation* reported that the cysteine proteinase allergen Der p 1 from fecal pellets of HDM can cause damage to the tight junction proteins *in vitro*, specifically the protein occludin, allowing HDM to freely cross the airway epithelial layer and suggesting this can contribute to allergic HDM sensitization (Wan et al., 1999). Two years later the same research group published a follow up study in *Clinical and Experimental Allergy* showing damage to the tight junction protein ZO-1 as well as occludin *in vitro* (but not to E-cadherin), resulting in epithelial permeability to mannitol (Wan et al., 2001). In an effort to reproduce these findings in an *in vivo* mouse model, Powdrill developed an HDM exposure protocol equivalent to that which produced epithelial damage in the two *in vitro* studies by Wan and colleagues. Surprisingly, Powdrill reported no change in epithelial barrier function when performing a ^{99m}Tc-DTPA lung clearance test in female BALB/c mice exposed to HDM. She repeated the experiment at a higher dose of HDM, at levels that have produced allergic asthma symptoms in established mouse models of asthma, with the same

results. The reason for this discrepancy between Powdrill's *in vivo* findings and the *in vitro* results in the Wan studies are unknown, but this difference in epithelial permeability models is similar to the differences we have observed in our study compared to previous *in vitro* work on goblet cells and epithelial permeability. While we do not know the exact mechanism that prevents the barrier dysfunction due to goblet cell metaplasia observed *in vitro*, these two studies serve as examples of the limited generalizability of *in vitro* results *to in vivo* systems. By isolating the airway epithelium *in vitro*, we are potentially preventing any preventative or restorative attempts by the body to act in response to the goblet cell metaplasia to keep barrier function intact. Therefore, the decreased transepithelial resistance measured in the *in vitro* study by Lachowicz-Scroggins and colleagues does not represent the same environment we examined in our *in vivo* model.

5.5.3 The Role of Specific Tight Proteins

Our study is limited in that we did not image or quantify tight junction proteins in the airway epithelium. We cannot directly confirm that tight junction proteins decreased in our model; we made this assumption based on the Matsumara and Steoguti paper that identified decreased tight junction proteins between goblet cells across various epithelia and the Lachowicz-Scroggins study that observed decreased transepithelial resistance after goblet cell metaplasia. Our study could be strengthened by imaging the airway epithelium from our

tissue slices with electron microscopy to obtain a representative image of the transepithelial structures, and to stain for the known airway epithelial tight junction proteins and quantify their expression in our study arms. It is possible that certain tight junction proteins are essential to maintain a specific level of epithelial integrity; despite the decrease in the total number of tight junction proteins between goblet cells, as long as certain key tight junction proteins remain epithelial integrity to certain particles is still maintained.

Tight junctions consist of many proteins including (but not limited to) claudins, occludin, and tricellulins, junctional adhesion molecules, and the cytoskeletal linker proteins zonula occludens (ZO)-1, ZO-2, and ZO-3 (Furuse, 2010). There is evidence that different expression of tight junction proteins are required depending on the function of the epithelia studied. It is important to note that our understanding of epithelia and of tight junction proteins do not always come from experiments examining the airway epithelium. Transepithelial resistance differs by several orders of magnitude depending on the tissue (e.g. airway, gallbladder, urinary bladder epithelium) and the species (e.g. mouse, rabbit, dog, human) studied (Anderson and Van Itallie, 2009). Tissues with different function likely require different expression of tight junction proteins, and therefore result in different transepithelial resistance, and cannot always be directly compared to the airway epithelium. For example, the epithelium in the human gastrointestinal tract is of low transepithelial resistance (except the distal colon) compared with other tissues such as the epithelium in the nephron

(Anderson and Van Itallie, 2009). This relatively leaky epithelium may be essential to allow the intestines to secrete and reabsorb the large amounts of fluid that passes through the system. It is likely that epithelia have specific arrangements of tight junction proteins that suit the function of the specific tissue. Therefore, transepithelial resistance may depend on the profile of the tight junction proteins, rather than their absolute number or the different cell types (i.e. ciliated epithelial cell or goblet cell) that they are anchored to (Anderson and Van Itallie, 2009). Evidence to support this theory can be found in the selectivity of relative leaky epithelia. Epithelia have been shown to allow passage of sodium ions (Na^+) over potassium ions (K^+), despite being of similar size and identical charge (Anderson and Van Itallie, 2009).

A study performed by Saitou and colleagues examined the role of the tight junction protein occludin and its role in barrier function (Saitou et al., 2000). It was previously though that occludin was a necessary tight junction protein to maintain epithelial barrier function (Chen et al., 1997). However, Saitou and colleagues bred an occludin knockout mouse (occludin -/-) that had no measurable intestinal epithelial barrier dysfunction (Saitou et al., 2000). While occludin may be essential in the epithelia of other tissues, or as a barrier to specific ions or molecules, this study highlights the diversity in tight junction proteins acting as a barrier. Therefore, specific tight junction proteins may act as a barrier to specific molecules.

In our study, although the number of tight junction proteins *may* have decreased, the remaining profile of tight junction protein types may be sufficient to prevent an aerosol the size of DTPA to freely pass the epithelial barrier. It would be of interest to compare the tight junction proteins in the epithelium of our mouse model to that of asthmatic patients and healthy controls to track the similarities and differences in tight junction profile; to help identify tight junction proteins sufficient to prevent the movement of DTPA across the epithelial barrier.

5.5.4 Relevency of the DTPA Lung Clearance Test

It is possible that there was a small amount of epithelial damage in our experiment that went undetected. The Lachowicz-Scroggins study that demonstrated epithelial permeability after goblet cell metaplasia *in vivo* measured transepithelial resistance; the movement of ions across the epithelium. We tracked the movement of the radio-labeled aerosol ^{99m}Tc-DTPA, which is much larger than most ions at 492 Daltons (Da) (Royston et al., 1990). Therefore it is possible that we were not able to detect small decreases in epithelial permeability; however, we believe changes of this magnitude would not be physiologically relevant.

We still believe the ^{99m}Tc-DTPA lung clearance test is a useful tool in asthma research. Our model in this study represents some IL-13 mediated asthma phenotypes (such as goblet cell metaplasia and airway hyperresponsiveness to nebulized methacholine) yet did not replicate epithelial

barrier dysfunction. Human asthmatics do have epithelial damage that allows ^{99m}Tc-DTPA to cross the epithelial barrier to a significant degree compared to healthy controls (Bhure et al., 2009). Damage to this extent may prevent the epithelium from acting as a protective barrier to allergens or irritants that normally do not have free access to the internal airway environment. The epithelial barrier in our model did not allow increased movement of DTPA compared to control, and therefore does not completely model the barrier dysfunction observed in human asthma.

5.6 Conclusions

Airway epithelial barrier dysfunction observed in asthma, likely a result of damaged or altered epithelial tight junction proteins, is believed to promote allergic sensitization and contribute to asthma exacerbations (Xiao et al., 2011). We believed this barrier dysfunction was due to the transformation of airway epithelial cells into goblet cells, due in part to a potential decrease in tight junction proteins. We created an *in vivo* mouse model using female BALB/c mice and overexpressed the Th2 cytokine IL-13 via an adenovirus vector to promote goblet cell metaplasia. We achieved increased goblet cell expression and airway hyperresponsiveness to nebulized methacholine, but did not show increased epithelial permeability to the radio labeled aerosol ^{99m}Tc-DTPA. This lung clearance test has modeled epithelial damage in other models in our lab, and has indicated significantly increased rates of clearance out of the airways in human

patients with asthma. While we did not quantify airway epithelial tight junction proteins, previous studies have indicated that the type rather than the absolute number of tight junction proteins may be essential to maintain epithelial barrier integrity. Based on our model, we conclude that IL-13 induced goblet cell metaplasia is insufficient to cause airway barrier dysfunction to ^{99m}Tc-DTPA.

5.7 Future Directions

While we believe our model had adequately shown that goblet cell metaplasia alone does not lead to an impaired epithelial barrier to DTPA, it would be interesting to follow-up with additional experiments to further elucidate airway epithelial permeability. ^{99m}Tc-DTPA was used in this study because asthmatic patients as well as animal models of asthma are significantly more permeable to this aerosol compared to control animals. However, it would be interesting to determine if our goblet cell metaplasia mouse model used in this study results in significantly greater permeability to other molecules smaller than DTPA. For example, histamine is a molecule that is physiologically relevant to asthma and is smaller than DTPA. If we can attach a label to histamine (or perhaps an inert particle of similar size) and administer it into the airways it would be of interest to compare its dispersion in a goblet cell metaplasia model compared to control. Our model only allows us to conclude that goblet cell metaplasia does not result in a leaky epithelium to molecules the size of DTPA or larger. With a labeled

histamine model, we can determine the permeability of a molecule much smaller than DTPA.

The model used in this experiment could also be optimized by manipulating the dose of adenovirus. A dose response curve could be obtained with the goal of achieving significantly increased number of goblet cells at the lowest possible dose of adenovirus, to minimize the other effects of IL-13 overexpression such as an influx of inflammatory cells.

Tight junction proteins are attributed to the ability of the airway epithelium to act as a barrier to molecules that would otherwise pass between two adjacent airway epithelial cells. Determining the tight junction profile of our epithelial goblet cell metaplasia model might help us understand why our model was not leaky to ^{99m}Tc-DTPA compared to the leaky epithelium observed in asthma models. A Western blot (protein immunoblot) could be performed to quantify the levels of tight junction proteins in the airway epithelium. However, if tight junctions are disrupted the proteins may remain loose in the intra-epithelial space, and therefore would be detected by Western blot despite not functioning as an intact barrier. Staining for specific tight junction proteins may be more helpful to quantify the tight junction proteins between epithelial cells in our goblet cell metaplasia mouse model.

CHAPTER 6: REFERENCES

Afshar R, Medoff BD, Luster AD. Allergic asthma: a tale of many T cells. *Clin Exp Allergy*. 2008;38(12):1847-57

Allahverdian S, Harada N, Singhera GK, Knight DA, Dorscheid DR. Secretion of IL-13 by airway epithelial cells enhances epithelial repair via HB-EGF. *Am J Respir Cell Mol Biol*. 2008;38(2):153-60

American Thoracic Society; European Respiratory Society. ATS/ERS recommendations for standardized procedures for the online and offline measurement of exhaled lower respiratory nitric oxide and nasal nitric oxide, 2005. *Am J Respir Crit Care Med*. 2005;171(8):912-30.

Anderson JM, Van Itallie CM. Physiology and function of the tight junction. *Cold Spring Harb Perspect Biol*. 2009;1(2):a002584.

Anderson SD. Provocative challenges to help diagnose and monitor asthma: exercise, methacholine, adenosine, and mannitol. *Curr Opin Pulm Med*. 2008;14(1):39-45

Andrews AL, Nordgren IK, Kirby I, Holloway JW, Holgate ST, Davies DE, Tavassoli A. Cytoplasmic tail of IL-13Ralpha2 regulates IL-4 signal transduction. *Biochem Soc Trans*. 2009;37(Pt 4):873-6.

Bacharier LB, Jabara H, Geha RS. Molecular mechanisms of immunoglobulin E regulation. *Int Arch Allergy Immunol*. 1998;115(4):257-69.

Bang LM, Plosker GL. Spotlight on omalizumab in allergic asthma. *BioDrugs*. 2004;18(6):415-8

Baraldi E, de Jongste JC; European Respiratory Society/American Thoracic Society (ERS/ATS) Task Force. Measurement of exhaled nitric oxide in children, 2001. *Eur Respir J*. 2002;20(1):223-37

Barbato A, Turato G, Baraldo S, Bazzan E, Calabrese F, Panizzolo C, Zanin ME, Zuin R, Maestrelli P, Fabbri LM, Saetta M. Epithelial damage and angiogenesis in the airways of children with asthma. *Am J Respir Crit Care Med*. 2006;174(9):975-81

Barnes PJ. Immunology of asthma and chronic obstructive pulmonary disease. *Nat Rev Immunol*. 2008;8(3):183-92

Barnes PJ, Dweik RA, Gelb AF, Gibson PG, George SC, Grasemann H, Pavord ID, Ratjen F, Silkoff PE, Taylor DR, Zamel N. Exhaled nitric oxide in pulmonary diseases: a comprehensive review. *Chest*. 2010;138(3):682-9

Bateman ED, Hurd SS, Barnes PJ, Bousquet J, Drazen JM, FitzGerald M, Gibson P, Ohta K, O'Byrne P, Pedersen SE, Pizzichini E, Sullivan SD, Wenzel SE, Zar HJ. Global strategy for asthma management and prevention: GINA executive summary. *Eur Respir J*. 2008;31(1):143-78

Bates JH, Rincon M, Irvin CG. Animal models of asthma. *Am J Physiol Lung Cell Mol Physiol*. 2009;297(3):L401-10

Bergeron C, Al-Ramli W, Hamid Q. Remodeling in asthma. *Proc Am Thorac Soc*. 2009;6(3):301-5.

Bhure UN, Bhure SU, Bhatt BM, Mistry S, Pednekar SJ, Chari VV, Desai SA, Joshi JM, Paidhungat AJ. Lung epithelial permeability and inhaled furosemide: added dimensions in asthmatics. *Ann Nucl Med*. 2009;23(6):549-57

Bloemen K, Verstraelen S, Van Den Heuvel R, Witters H, Nelissen I, Schoeters G. The allergic cascade: review of the most important molecules in the asthmatic lung. *Immunol Lett*. 2007;31;113(1):6-18

Bochner BS, Klunk DA, Sterbinsky SA, Coffman RL, Schleimer RP. IL-13 selectively induces vascular cell adhesion molecule-1 expression in human endothelial cells. *J Immunol*. 1995;154(2):799-803

Boulet LP, Laviolette M, Turcotte H, Cartier A, Dugas M, Malo JL, Boutet M. Bronchial subepithelial fibrosis correlates with airway responsiveness to methacholine. *Chest*. 1997;112(1):45-52.

Bradding P, Walls AF, Holgate ST. The role of the mast cell in the pathophysiology of asthma. *J Allergy Clin Immunol*. 2006;117(6):1277-84

Braman SS. The global burden of asthma. *Chest*. 2006;130:4S–12S

Brightling CE. Clinical applications of induced sputum. *Chest*. 2006 May;129(5):1344-8

Busse WW, Lemanske RF. Asthma. *N Engl J Med*. 2001;344(5):350-62

Busse WW, Ring J, Huss-Marp J, Kahn JE. A review of treatment with mepolizumab, an anti-IL-5 mAb, in hypereosinophilic syndromes and asthma. *J Allergy Clin Immunol*. 2010;125(4):803-13

Chen Y, Merzdorf C, Paul DL, Goodenough DA. COOH terminus of occludin is required for tight junction barrier function in early Xenopus embryos. *J Cell Biol*. 1997;138(4):891-9.

Chen Z, Jin N, Narasaraju T, Chen J, McFarland LR, Scott M, Liu L. Identification of two novel markers for alveolar epithelial type I and II cells. *Biochem Biophys Res Commun*. 2004;319(3):774-80.

Claude P, Goodenough DA. Fracture faces of zonulae occludentes from "tight" and "leaky" epithelia. *J Cell Biol*. 1973;58(2):390-400.

Cockcroft DW, Davis BE. Mechanisms of airway hyperresponsiveness. *J Allergy Clin Immunol*. 2006;118(3):551-9

Cockcroft DW, McParland CP, Britto SA, Swystun VA, Rutherford BC. Regular inhaled salbutamol and airway responsiveness to allergen. *Lancet*. 1993;342(8875):833-7

Cohen J, Postma DS, Douma WR, Vonk JM, De Boer AH, Ten Hacken NH. Particle size matters: diagnostics and treatment of small airways involvement in asthma. *Eur Respir J*. 2011;37(3):532-40

Cromwell O, Hamid Q, Corrigan CJ, Barkans J, Meng Q, Collins PD, Kay AB. Expression and generation of interleukin-8, IL-6 and granulocyte-macrophage colony-stimulating factor by bronchial epithelial cells and enhancement by IL-1 beta and tumour necrosis factor-alpha. *Immunology*. 1992;77(3):330-7

Crosby LM, Waters CM. Epithelial repair mechanisms in the lung. *Am J Physiol Lung Cell Mol Physiol*. 2010;298(6):L715-31

Davies DE. The bronchial epithelium in chronic and severe asthma. *Curr Allergy Asthma Rep*. 2001;1(2):127-33

Davis BE, Illamperuma C, Gauvreau GM, Watson RM, O'Byrne PM, Deschesnes F, Boulet LP, Cockcroft DW. Single-dose desloratadine and montelukast and allergen-induced late airway responses. *Eur Respir J*. 2009;33(6):1302-8

Davis CW, Dickey BF. Regulated airway goblet cell mucin secretion. *Annu Rev Physiol*. 2008;70:487-51

Efthimiadis A, Spanevello A, Hamid Q, Kelly MM, Linden M, Louis R, Pizzichini MM, Pizzichini E, Ronchi C, Van Overvel F, Djukanović R. Methods of sputum processing for cell counts, immunocytochemistry and in situ hybridisation. *Eur Respir J Suppl*. 2002;37:19s-23s

Elias JA, Zhu Z, Chupp G, Homer RJ. Airway remodeling in asthma. *J Clin Invest*. 1999;104(8):1001-6

Epstein MM. Do mouse models of allergic asthma mimic clinical disease? *Int Arch Allergy Immunol*. 2004;133(1):84-100

Erlander MG, Tillakaratne NJ, Feldblum S, Patel N, Tobin AJ. Two genes encode distinct glutamate decarboxylases. *Neuron*. 1991;7(1):91-100.

Farquhar MG, Palade GE. Junctional complexes in various epithelia. *J Cell Biol*. 1963;17:375-412

Foster PS, Hogan SP, Ramsay AJ, Matthaei KI, Young IG. Interleukin 5 deficiency abolishes eosinophilia, airways hyperreactivity, and lung damage in a mouse asthma model. *J Exp Med*. 1996;183(1):195-201

Furuse M. Molecular basis of the core structure of tight junctions. *Cold Spring Harb Perspect Biol*. 2010;2(1):a002907

Galli SJ. Complexity and redundancy in the pathogenesis of asthma: reassessing the roles of mast cells and T cells. *J Exp Med*. 1997;186(3):343-7.

Gardner A, Borthwick LA, Fisher AJ. Lung epithelial wound healing in health and disease. *Expert Rev Respir Med*. 2010;4(5):647-60

Godfrey RW. Human airway epithelial tight junctions. *Microsc Res Tech*. 1997;38(5):488-99

Grainge CL, Lau LC, Ward JA, Dulay V, Lahiff G, Wilson S, Holgate S, Davies DE, Howarth PH. Effect of bronchoconstriction on airway remodeling in asthma. *N Engl J Med*. 2011;364(21):2006-15

Gumbiner B. Structure, biochemistry, and assembly of epithelial tight junctions. *Am J Physiol*. 1987;253(6 Pt 1):C749-58

Hajoui O, Janani R, Tulic M, Joubert P, Ronis T, Hamid Q, Zheng H, Mazer BD. Synthesis of IL-13 by human B lymphocytes: regulation and role in IgE production. *J Allergy Clin Immunol*. 2004;114(3):657-63.

Haraguchi M, Shimura S, Shirato K. Morphometric analysis of bronchial cartilage in chronic obstructive pulmonary disease and bronchial asthma. *Am J Respir Crit Care Med*. 1999;159(3):1005-13.

Hargreave FE. Quantitative sputum cell counts as a marker of airway inflammation in clinical practice. *Curr Opin Allergy Clin Immunol*. 2007;7(1):102-6

Hedblom E, Kirkness EF. A novel class of GABAA receptor subunit in tissues of the reproductive system. *J Biol Chem*. 1997;272(24):15346-50

Hershey GK. IL-13 receptors and signaling pathways: an evolving web. *J Allergy Clin Immunol*. 2003;111(4):677-90

Holgate ST. Epithelium dysfunction in asthma. *J Allergy Clin Immunol*. 2007;120(6):1233-44

Holgate ST. Pathogenesis of Asthma. *Clin Exp Allergy*. 2008;38(6):872-97

Ilowite JS, Bennett WD, Sheetz MS, Groth ML, Nierman DM. Permeability of the bronchial mucosa to 99mTc-DTPA in asthma. *Am Rev Respir Dis*. 1989;139(5):1139-43

Jeffery PK, Wardlaw AJ, Nelson FC, Collins JV, Kay AB. Bronchial biopsies in asthma. An ultrastructural, quantitative study and correlation with hyperreactivity. *Am Rev Respir Dis*. 1989;140(6):1745-53.

Jin N, Narasaraju T, Kolliputi N, Chen J, Liu L. Differential expression of GABAA receptor pi subunit in cultured rat alveolar epithelial cells. *Cell Tissue Res*. 2005;321(2):173-83

Kaplan AG, Balter MS, Bell AD, Kim H, McIvor RA. Diagnosis of asthma in adults. *CMAJ*. 2009;181(10):E210-20

Kucharzik T, Walsh SV, Chen J, Parkos CA, Nusrat A. Neutrophil transmigration in inflammatory bowel disease is associated with differential expression of epithelial intercellular junction proteins. *Am J Pathol*. 2001;159(6):2001-9

Kuperman DA, Schleimer RP. Interleukin-4, interleukin-13, signal transducer and activator of transcription factor 6, and allergic asthma. *Curr Mol Med*. 2008;8(5):384-92

Kuwano K, Bosken CH, Paré PD, Bai TR, Wiggs BR, Hogg JC. Small airways dimensions in asthma and in chronic obstructive pulmonary disease. *Am Rev Respir Dis*. 1993;148(5):1220-5.

Lachowicz-Scroggins ME, Boushey HA, Finkbeiner WE, Widdicombe JH. Interleukin-13-induced mucous metaplasia increases susceptibility of human airway epithelium to rhinovirus infection. *Am J Respir Cell Mol Biol*. 2010;43(6):652-61

Laoukili J, Perret E, Willems T, Minty A, Parthoens E, Houcine O, Coste A, Jorissen M, Marano F, Caput D, Tournier F. IL-13 alters mucociliary differentiation and ciliary beating of human respiratory epithelial cells. *J Clin Invest*. 2001;108(12):1817-24.

Leigh R, Vethanayagam D, Yoshida M, Watson RM, Rerecich T, Inman MD, O'Byrne PM. Effects of montelukast and budesonide on airway responses and airway inflammation in asthma. *Am J Respir Crit Care Med*. 2002;166(9):1212-7

Lemanske RF, Busse WW. Asthma. *J Allergy Clin Immunol*. 2003;111(2):S502-19

Leonard EJ, Yoshimura T. Neutrophil attractant/activation protein-1 (NAP-1 [interleukin-8]). *Am J Respir Cell Mol Biol*. 1990;2(6):479-86

Li X, Wilson JW. Increased vascularity of the bronchial mucosa in mild asthma. *Am J Respir Crit Care Med*. 1997;156(1):229-33.

Lu WY, Inman MD. Gamma-aminobutyric acid nurtures allergic asthma. *Clin Exp Allergy*. 2009;39(7):956-61

Martin DL, Rimvall K. Regulation of gamma-aminobutyric acid synthesis in the brain. *J Neurochem*. 1993;60(2):395-407

Masoli M, Fabian D, Holt S, and Beasley R. The global burden of asthma: executive summary of the GINA Dissemination Committee Report. *Allergy*. 2004;59:469–78

Matsumura H, Setoguti T. Freeze-fracture replica studies of tight junctions in normal human bronchial epithelium. *Acta Anat (Basel)*. 1989;134(3):219-26

Meyers DA. Genetics of asthma and allergy: what have we learned? *J Allergy Clin Immunol*. 2010;126(3):439-46

Miller MR, Hankinson J, Brusasco V, Burgos F, Casaburi R, Coates A, Crapo R, Enright P, van der Grinten CP, Gustafsson P, Jensen R, Johnson DC, MacIntyre N, McKay R, Navajas D, Pedersen OF, Pellegrino R, Viegi G, Wanger J; ATS/ERS Task Force. Standardisation of spirometry. *Eur Respir J*. 2005;26(2):319-38.

Montefort S, Roberts JA, Beasley R, Holgate ST, Roche WR. The site of disruption of the bronchial epithelium in asthmatic and non-asthmatic subjects. *Thorax*. 1992;47(7):499-503

Nash S, Stafford J, Madara JL. The selective and superoxide-independent disruption of intestinal epithelial tight junctions during leukocyte transmigration. *Lab Invest*. 1988;59(4):531-7

O'Byrne PM. Allergen-induced airway inflammation and its therapeutic intervention. *Allergy Asthma Immunol Res*. 2009;1(1):3-9

O'Byrne PM, Inman MD. Airway hyperresponsiveness. *Chest*. 2003;123(3):411S-6S

Persson MG, Zetterström O, Agrenius V, Ihre E, Gustafsson LE. Single-breath nitric oxide measurements in asthmatic patients and smokers. *Lancet*. 1994;343(8890):146-7.

Pelaia G, Renda T, Gallelli L, Vatrella A, Busceti MT, Agati S, Caputi M, Cazzola M, Maselli R, Marsico SA. Molecular mechanisms underlying airway smooth muscle contraction and proliferation: implications for asthma. *Respir Med*. 2008;102(8):1173-81

Peters SP, Kunselman SJ, Icitovic N, Moore WC, Pascual R, Ameredes BT, Boushey HA, Calhoun WJ, Castro M, Cherniack RM, Craig T, Denlinger L, Engle LL, DiMango EA, Fahy JV, Israel E, Jarjour N, Kazani SD, Kraft M, Lazarus SC, Lemanske RF Jr, Lugogo N, Martin RJ, Meyers DA, Ramsdell J, Sorkness CA, Sutherland ER, Szefler SJ, Wasserman SI, Walter MJ, Wechsler ME, Chinchilli VM, Bleecker ER; National Heart, Lung, and Blood Institute Asthma Clinical Research Network. Tiotropium bromide step-up therapy for adults with uncontrolled asthma. *N Engl J Med*. 2010;363(18):1715-26

Proud D, Leigh R. Epithelial cells and airway diseases. *Immunol Rev*. 2011;242(1):186-204

Ramshaw I, Ruby J, Ramsay A, Ada G, Karupiah G. Expression of cytokines by recombinant vaccinia viruses: a model for studying cytokines in virus infections in vivo. *Immunol Rev*. 1992;127:157-82.

Rees J. Asthma control in adults. *BMJ*. 2006;332(7544):767-71

Rogers DF. The airway goblet cell. *Int J Biochem Cell Biol*. 2003;35(1):1-6

Rosenberg HF, Phipps S, Foster PS. Eosinophil trafficking in allergy and asthma. *J Allergy Clin Immunol*. 2007;119(6):1303-10

Rothenberg ME, Hogan SP. The eosinophil. *Annu Rev Immunol*. 2006;24:147-74

Royston BD, Webster NR, Nunn JF. Time course of changes in lung permeability and edema in the rat exposed to 100% oxygen. *J Appl Physiol*. 1990;69(4):1532-7

Saitou M, Furuse M, Sasaki H, Schulzke JD, Fromm M, Takano H, Noda T, Tsukita S. Complex phenotype of mice lacking occludin, a component of tight junction strands. *Mol Biol Cell*. 2000;11(12):4131-42

Saunders KB. Origin of the word “asthma”. *Thorax*. 1993;48:647

Sime PJ, Xing Z, Graham FL, Csaky KG, Gauldie J. Adenovector-mediated gene transfer of active transforming growth factor-beta1 induces prolonged severe fibrosis in rat lung. *J Clin Invest*. 1997;100(4):768-76

Skadhauge LR, Christensen K, Kyvik KO, Sigsgaard T. Genetic and environmental influence on asthma: a population-based study of 11,688 Danish twin pairs. *Eur Respir J*. 1999;13(1):8-14

Shinagawa K, Kojima M. Mouse model of airway remodeling: strain differences. *Am J Respir Crit Care Med*. 2003;168(8):959-67

Shore SA. Direct effects of Th2 cytokines on airway smooth muscle. *Curr Opin Pharmacol*. 2004;4(3):235-40

Soumelis V, Reche PA, Kanzler H, Yuan W, Edward G, Homey B, Gilliet M, Ho S, Antonenko S, Lauerma A, Smith K, Gorman D, Zurawski S, Abrams J, Menon S, McClanahan T, de Waal-Malefyt Rd R, Bazan F, Kastelein RA, Liu YJ. Human epithelial cells trigger dendritic cell mediated allergic inflammation by producing TSLP. *Nat Immunol*. 2002;3(7):673-80

Southam DS, Ellis R, Wattie J, Young S, Inman MD. Budesonide prevents but does not reverse sustained airway hyperresponsiveness in mice. *Eur Respir J*. 2008;32(4):970-8

Turi GJ, Ellis R, Wattie JN, Labiris NR, Inman MD. The effects of inhaled house dust mite on airway barrier function and sensitivity to inhaled methacholine in mice. *Am J Physiol Lung Cell Mol Physiol*. 2011;300(2):L185-90

Venkayya R, Lam M, Willkom M, Grünig G, Corry DB, Erle DJ. The Th2 lymphocyte products IL-4 and IL-13 rapidly induce airway hyperresponsiveness through direct effects on resident airway cells. *Am J Respir Cell Mol Biol*. 2002;26(2):202-8

Vinkers CH, Mirza NR, Olivier B, Kahn RS. The inhibitory GABA system as a therapeutic target for cognitive symptoms in schizophrenia: investigational agents in the pipeline. *Expert Opin Investig Drugs*. 2010;19(10):1217-33

Voynow JA, Rubin BK. Mucins, mucus, and sputum. *Chest*. 2009;135(2):505-12

Wan H, Winton HL, Soeller C, Taylor GW, Gruenert DC, Thompson PJ, Cannell MB, Stewart GA, Garrod DR, Robinson C. The transmembrane protein occludin of epithelial tight junctions is a functional target for serine peptidases from faecal pellets of Dermatophagoides pteronyssinus. *Clin Exp Allergy*. 2001;31(2):279-94

Wan H, Winton HL, Soeller C, Tovey ER, Gruenert DC, Thompson PJ, Stewart GA, Taylor GW, Garrod DR, Cannell MB, Robinson C. Der p 1 facilitates transepithelial allergen delivery by disruption of tight junctions. J Clin Invest. 1999;104(1):123-33

Warner SM, Knight DA. Airway modeling and remodeling in the pathogenesis of asthma. *Curr Opin Allergy Clin Immunol*. 2008;8(1):44-8.

Wegmann M. Targeting Eosinophil's Biology in Asthma Therapy. *Am J Respir Cell Mol Biol*. 2011 [Epub ahead of print]

Xiang YY, Wang S, Liu M, Hirota JA, Li J, Ju W, Fan Y, Kelly MM, Ye B, Orser B, O'Byrne PM, Inman MD, Yang X, Lu WY. A GABAergic system in airway epithelium is essential for mucus overproduction in asthma. *Nat Med*. 2007;13(7):862-7

Xiao C, Puddicombe SM, Field S, Haywood J, Broughton-Head V, Puxeddu I, Haitchi HM, Vernon-Wilson E, Sammut D, Bedke N, Cremin C, Sones J, Djukanović R, Howarth PH, Collins JE, Holgate ST, Monk P, Davies DE. Defective epithelial barrier function in asthma. *J Allergy Clin Immunol*. 2011;128(3):549-556.e12

Xing Z, Braciak T, Jordana M, Croitoru K, Graham FL, Gauldie J. Adenovirus-mediated cytokine gene transfer at tissue sites. Overexpression of IL-6 induces lymphocytic hyperplasia in the lung. *J Immunol*. 1994;153(9):4059-69

Ying S, O'Connor B, Ratoff J, Meng Q, Mallett K, Cousins D, Robinson D, Zhang G, Zhao J, Lee TH, Corrigan C. Thymic stromal lymphopoietin expression is increased in asthmatic airways and correlates with expression of Th2-attracting chemokines and disease severity. *J Immunol*. 2005;174(12):8183-90

Zhu Z, Homer RJ, Wang Z, Chen Q, Geba GP, Wang J, Zhang Y, Elias JA. Pulmonary expression of interleukin-13 causes inflammation, mucus hypersecretion, subepithelial fibrosis, physiologic abnormalities, and eotaxin production. *J Clin Invest*. 1999;103(6):779-88.